

FPGA BASED CONTROLLER FOR FUEL CELL

A thesis submitted in partial fulfillment
Of the requirements for the degree of

Master of Technology

By

SUMIT KUMAR SAO

Roll No: 210EC2286

M. Tech 4th Sem

VLSI DESIGN AND EMBEDDED SYSTEMS

Under the guidance of

Prof. KAMALAKANTA MAHAPATRA



Department of Electronics and Communication Engineering

National Institute of Technology, Rourkela

May, 2012



Department of Electronics & Communication
Engineering
National Institute of Technology
Rourkela-769008

CERTIFICATE

This is to certify that the thesis entitled “**FPGA based Controller for Fuel Cell**” submitted by **Mr. Sumit Kumar Sao** in partial fulfillment of the requirements for the award of **Master of Technology** Degree in **Electronics and communication Engineering** with specialization in “**VLSI Design and Embedded Systems**” during session 2010-2012 at **National Institute of Technology, Rourkela** is an authentic work carried out by him under my supervision and guidance.

To the best of my knowledge, the matter embodied in the thesis has not been submitted to any other University / Institute for the award of any Degree or Diploma.

Date :

Place :

Prof. KamalaKanta Mahapatra

Dept. of Electronics & Communication Engineering
National Institute of Technology
Rourkela 769008

Acknowledgement

I would like to express my gratitude to my thesis guide **Prof. KAMALAKANTA MAHAPATRA** for his guidance, advice and constant support throughout my thesis work. I would like to thank him for being my advisor here at National Institute of Technology, Rourkela.

Next, I want to express my respects to **Prof. A. K. Swain, Mr. Kahnu Charan Bhuyan (Ph.D Scholar) and Mr. P. Karupanan (Ph.D Scholar)**, for teaching me and also helping me how to learn. They have been great sources of inspiration to me and I thank them from the bottom of my heart.

I would like to thank all faculty members and staff of the Department of Electronics and Communication Engineering, N.I.T. Rourkela for their generous help in various ways for the completion of this thesis.

I would like to thank all my friends and especially my classmates for all the thoughtful and mind stimulating discussions we had, which prompted us to think beyond the obvious. I've enjoyed their companionship so much during my stay at NIT, Rourkela.

I am especially indebted to my parents for their love, sacrifice, and support. They are my first teachers after I came to this world and have set great examples for me about how to live, study, and work.

SUMIT KUMAR SAO

Roll No: 210EC2286

Dept. of ECE

NIT Rourkela

ABSTRACT

This dissertation presents a fuel cell controller. A model is developed for Fuel Cell. We mainly deal the control of the fuel cell under a variety of different parameters, and implementation of the control system in an FPGA using VHDL. The output voltage of Fuel Cell is controlled or conditioned by some controllers; it may be digital or analog. Recently, the importance of the PWM has increased as it became an integral part of all the electronics system. There are two basic techniques for PWM generation, analog and digital. The disadvantages of the analog methods are that they are prone to noise, and they change with voltage and temperature change, they suffer changes due to component variation. To overcome the problem, associated with the analog technique, various types of digital technique are available. Implementation of these techniques in VHDL is done.

Keywords: - PEM Fuel cell, DC-DC Converter, PI Controller, PWM, FPGA, VHDL.

Table of Contents

Acknowledgement	iii
ABSTRACT.....	iv
List of figure	vii
List of table.....	ix
Chapter 1 INTRODUCTION	2
Chapter 2 : FUEL CELL	5
2.1 Types of Renewable Energy	5
2.2 Working Principle of Fuel cell.....	6
2.3 Types of Fuel cells	8
2.4 Modelling of a Fuel cell	9
2.5 Voltage-Current Polarization curve of fuel cell stack	14
2.6 Summary	15
Chapter 3 : DC-DC CONVERTER.....	17
3.1 Introduction.....	17
3.2 Types of DC-DC converter	18
3.2.1 Step-down (buck) converter:.....	19
3.2.2 Step-up (boost) converter:	22
3.2.3 Buck-Boost converter:.....	27
3.3 Simulation	30
3.4 Summary	33
Chapter 4 : CONTROL STRATEGY	35
4.1 Introduction	35
4.2 PWM (Pulse Width Modulation) Scheme	35
4.2.1 FPGA Implementation of PWM	37
4.2.2 Design Summary	38
4.4 Proportional Integral Control	39
4.4.1 FPGA Implementation of PI controller	40
4.4.2 Design Summary	42
4.5 FPGA implementation of PI and PWM.....	42

4.5.1 SPI interface signals of Amplifier to FPGA	44
4.5.2 State diagram to configure Amplifier gain	45
4.5.3 SPI interface signals of ADC	46
4.5.4 FSM State diagram to interface ADC with FPGA.....	47
4.5.5 RTL schematic of ADC Module.....	49
4.5.6 Verification of signal using Chipscope pro	50
4.6 ADC-DAC MODULE	50
4.6.1 RTL schematic of ADC-DAC module	51
4.6.2 Experimental set-up of ADC-DAC.....	52
4.7 Controller for Fuel Cell Power System.....	53
4.7.1 Analysis of PI and PWM with ADC using Chipscope Pro	53
4.7.2 Design summary of PI and PWM using ADC	54
4.7.3 Experimental set-up	54
4.8 Summary	54
Chapter 5 : HARDWARE IMPLEMENTATION OF FUEL CELL CONTROLLER	56
5.1 Sub block of PCU (Power Conditioning Unit).....	57
5.1.1 Subtractor Circuit:.....	57
5.1.2 Limiter (or Clipper) Circuit	58
5.1.3 Driver Circuit.....	59
5.3 Experimental Set-up	61
5.4 Summary	62
Chapter 6 CONCLUSION.....	63
Chapter 7 FUTURE WORK.....	64
Chapter 8 REFERENCES	65

List of figures

Figure 2.1 Basic working model of fuel cell.....	7
Figure 2.2 Simulink model of fuel cell.....	13
Figure 2.3 Fuel cell polarization curve	14
Figure 3.1 Buck converter circuit diagram	19
Figure 3.2 Inductor Current of buck converter during On and Off period	20
Figure 3.3 Plot of gain verses duty cycle.....	22
Figure 3.4 Boost converter circuit diagram	23
Figure 3.5 Boost converter during On period of switching pulse	23
Figure 3.6 Boost converter during Off period of switching pulse.....	24
Figure 3.7 Inductor current of Boost converter.....	25
Figure 3.8 Plot of gain verses duty cycle of boost converter	26
Figure 3.9 Buck-boost converter circuit diagram.....	27
Figure 3.10 Buck-boost converter when switch closed	28
Figure 3.11 Inductor current of buck-boost converter	28
Figure 3.12 Simulink model buck converter.....	30
Figure 3.13 Output waveform of buck converter	30
Figure 3.14 Simulink model of boost converter.....	31
Figure 3.15 Output waveform of boost converter	31
Figure 3.16 Simulink model of buck-boost converter	32
Figure 3.17 Output waveform of buck-boost converter.....	32
Figure 4.1 Block diagram PWM signal generation	36
Figure 4.2 PWM Duty cycle control diagram	36
Figure 4.3 Entity of PWM	37
Figure 4.4 RTL schematic of PWM	38
Figure 4.5 Test bench waveform of PWM.....	38
Figure 4.6 Entity of PI controller	40
Figure 4.7 RTL schematic of PI controller	41
Figure 4.8 Test bench waveform of PI controller.....	41

Figure 4.9. Analog capture circuit in Spartan 3E board	43
Figure 4.10 SPI signal interface to amplifier	44
Figure 4.11 Timing diagram of amplifier	45
Figure 4.12 FSM for setting gain of amplifier	46
Figure 4.13 SPI signal interface of ADC	47
Figure 4.14 Timing diagram of ADC SPI signal.....	47
Figure 4.15 FSM for getting data from ADC.....	48
Figure 4.16 RTL schematic of ADC (part 1)	49
Figure 4.17 RTL schematic of ADC (part 2)	49
Figure 4.18 Chipscope pro analysis of internal signal of ADC.....	50
Figure 4.19 Entity of top level module	51
Figure 4.20 RTL schematic of TOP_level module	51
Figure 4.21 RTL schematic of Main_cntrl	52
Figure 4.22 Experimental set-up for ADC-DAC	52
Figure 4.24 PWM out signal analysis using chipscope pro	53
Figure 4.23 Block diagram of controller for Fuel cell	53
Figure 4.25 Experimental set-up for PI and PWM using ADC.....	54
Figure 5.1 Power conditioning unit for fuel cell	56
Figure 5.2 Op-amp based subtractor circuit.....	58
Figure 5.3 Schematic diagram of Limiter circuit	58
Figure 5.4 Waveform output of Limiter circuit.....	59
Figure 5.5 Opto Coupler internal schematic of (HCPL817)	60
Figure 5.6 Complete circuit for fuel cell.....	61

List of tables

Table 2.1 Comparison of different generation systems	6
Table 4.1 Design summary of PWM	38
Table 4.2 Design summary of PI controller	42
Table 4.4.3 Programmable Gain of Pre-amplifier	43
Table 4.4 SPI interface signals.....	44
Table 4.5 Design summary of PI and PWM using ADC	54

Chapter 1

Introduction

Chapter 1 INTRODUCTION

The ever increasing energy consumption in the modern world with the increased environmental issues has created interest in the field of renewable energy systems, which can meet the needs in residential/grid-connected system, transportation, industries and commercial applications. The renewable energy source comes with different cost and efficiency. The best among the all in cost of maintenance and high efficiency is the FUEL CELL. It has several advantages over others.

The power generated by the fuel cell is not suitable to use directly in any application. We need to condition it by using some power conditioning units. The fuel cell voltage is converted directly into AC supply by using a single stage DC/AC inverter topologies or by two stages (DC/DC converter in conjunction with a DC / AC inverter).

The converter stages are to be controlled to give the desired output power in a different real world environment, which can either be accomplished by hard switching techniques or by using digital controller. PWM technique has become an integral part of all the electronic system. This technique has many salient features, due to which it replaced the traditional use of digitally on-off signal to control the switching action of the converter. A controller which minimizes the error and brings the close loop system to stability is done using a PI controller which is easy to tune. Implementation of these techniques in VHDL is done. The controller is implemented in FPGA.

Controller designed in an FPGA has to be interfaced to a power circuit which needs an isolation and Analog to digital converter for analog input to digital controllers. Using on-board ADC of Spartan 3E board error signal is fed to PI controller. ADC LTC1407 is an SPI

interfacing with FPGA; which needs a module which generates SPI signals to communicate with the FPGA. A hardware prototype for the fuel cell controller is made and a 12 V 500 mA power system is designed.

Chapter 2

Fuel Cell

Chapter 2 : FUEL CELL

In this fast, modernizing world and exponentially increasing population with the ongoing fully automation world, the need of the energy is also increasing. Due to the limited source and increasing pricing of the non-renewable energy along with the global environment issue, this is raising public awareness of environmental protection. We need to fulfill the energy requirement with keeping in mind about the environmental issue only possible is to start using more and more renewable energy sources.

2.1 Types of Renewable Energy

1. Solar Energy
2. Wind Energy
3. Bio-energy
4. Hydropower
5. Ocean Energy
6. Hydrogen & Fuel Cells

We have a good number of renewable energy sources with different specification and ability. These can be the small-scale generation systems which can be used as an alternative energy source for different purpose. One which is now most attracted and potential source is Fuel cells.

Fuel cells are static energy generation devices which convert the chemical reaction of fuels supplied to it directly into electrical energy. It is also good in the sense of environmental protection as its byproduct is water and heat [1]. Some Fuel cells produce large amount of heat which again can be used to generate electricity and increase its efficiency. While, other

conventional heat engines produce electricity from chemical energy with the use of intermediate mechanical energy conversion which results in reduced efficiency compared with fuel cells. It combines the best of the engines and battery; generates energy till fuels is available without any intermediate mechanical energy conversion and behave as battery under load condition.

Table 2.1 Comparison of different generation systems

	Reciprocating engine: diesel	Turbine generator	Photo voltaic	Wind turbine	Fuel cells
Capacity Range(W)	500 k to 5 M	500 k to 25M	1 k to 1M	10 k to 1 M	200 k to 2 M
Efficiency (%)	35	29–42	6–19	25	40–60
Capital Cost (\$/kW)	200–350	450–870	6600	1000	1500–3000
O&M Cost (\$/kW)	0.005–0.015	0.005–0.0065	0.001–0.004	0.01	0.0019–0.0153

Table 1 shows a comparison of different generation systems. It is observed that the efficiency of fuel cells has been always higher as compared with conventional systems and other distributed generation systems. Fuel cell offers more advantages over other distributed generation technologies, like high energy conversion efficiency, zero emission, modularity, scalability and gives good opportunities for cogeneration operations [1]. It is clear that Fuel cell is a good option for distributed generation systems.

2.2 Working principle of Fuel cell

The fuel cell is a static device that converts the chemical energy directly into electricity with byproduct water and heat. A simplified fuel cell working is shown in Fig. 1 [3]. It consists of an electrolyte layer in contact with two electrodes. In which one is fueled with hydrogen fuel and other with oxygen. It acts as an anode electrode and a cathode electrode respectively. The fuel

and oxidant is to be fed continuously. The electrolyte which acts like a membrane permits only the positive ions to flow from anode to cathode and acts as an insulator for electrons. The electron produced from the hydrogen fuel after it decomposed tries to get stable by going to cathode side which is accomplished by an external circuit. And this way an electricity is generated. The reaction takes place in the fuel cell are

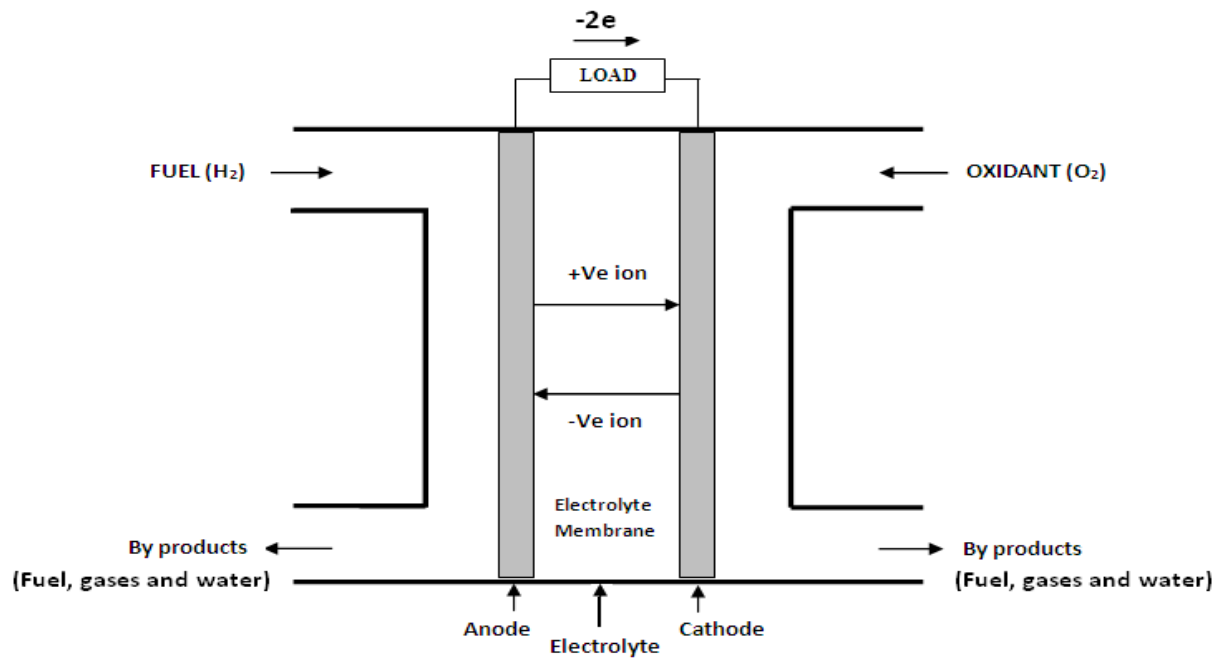
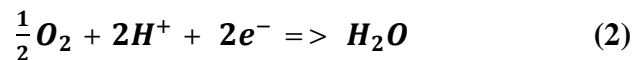


Figure 2.1 Basic working model of fuel cell

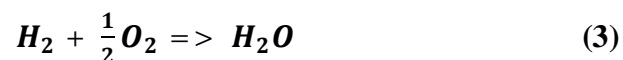
Anode reaction:



Cathode reaction:



Overall reaction:



2.3 Types of Fuel cells

The fuel cells are categories according to the type of electrolyte and fuel its use.

1. Proton exchange membrane fuel cell (PEMFC):
2. Alkaline fuel cell (AFC):
3. Phosphoric acid fuel cell (PAFC)
4. Molten carbonate fuel cell (MCFC)
5. Solid oxide fuel cell (SOFC)
6. Direct methanol fuel cell (DMFC)

They can also be classified on their operating temperature, low operating temperature fuel cell is PEMFC, AFC and PAFC, and high operating temperature like MCFC and SOFC. The PEM fuel cell uses a solid polymer electrolyte to exchange the ions between two porous electrodes, which is a good conductor of protons and an insulator for electrons. The advantages are its higher power density and quick start up [4]. The major drawbacks are its lower operating efficiency (40-45%) and use of high cost platinum catalyst. Alkaline fuel cell (AFC) is like a PEM fuel cell and it has the capability to reach 60-70% of efficiency. It uses an aqueous solution of the potassium hydroxide as an electrolyte. This fuel cell gives quick start, one of its advantages. The major disadvantage is, it is very sensitive to CO_2 . It needs a separate system to remove the CO_2 from the air. The use of a corrosive electrolyte is also a disadvantage because it has a shorter life span. Phosphoric acid fuel cell (PAFC) operating temperature is almost double as compared to that of PEM fuel cell. It utilizes a liquid phosphoric acid as an electrode [5]. The drawback of PAFC is same as PEM fuel cell. The Molten Carbonate fuel cell consists of two porous electrodes with good conductivity are in contact with a molten carbonate cell. Due to its

internal reforming capability, it separates the hydrogen from the carbon monoxide fuel and decomposition of hydrogen is taken through the water shift reaction to produce hydrogen. The major advantages of MCFC are higher efficiency as 50-60%, no need of metal catalyst and separate reformer due to its high operating temperature. The SOFC uses dense yttria stabilized Zirconia, which is a solid ceramic material as its electrolyte. Here oxygen O^- combines with hydrogen H^+ to generate water and heat. The SOFC produces electricity at a high operating temperature of about 1000°C . The main advantages of the SOFC are that they operate at high efficiency of 50-60% and a separate reformer is not required to extract hydrogen from the fuel due to its internal reforming capability. Waste heat can be recycled to make additional electricity by cogeneration operation [5]. The slow start up, high cost and intolerant to the sulfur content of the fuel cell are some of its drawbacks.

2.4 Modelling of a Fuel cell

The FC model used in the thesis is developed in MATLAB/SIMULINK. This model has been built using the relationship between output voltage and partial pressure of hydrogen, oxygen and water. Fig. 2.2 shows the detailed model of the PEMFC, which is then embedded into the SimPowerSystems of MATLAB as a controlled source and integrated into the overall system. The FC system model parameters used to obtain this model are as follows:

β, C – Constants to simulate the activation over voltage in the FC system (A^{-1}) and (V)

E – Nernst instantaneous voltage (V)

E_O – Standard no load voltage (V)

F – Faraday's constants ($C(Kmol)^{-1}$)

I_{FC} – FC system current (A)

K_{an} – Anode valve constant ($\sqrt{kmolkg(atms)^{-1}}H_2O$)

K_H – Hydrogen valve molar constant ($kmol (atm s)^{-1}$)

K_{H_2O} – Water valve molar constant ($kmol (atm s)^{-1}$)

K_{O_2} – Oxygen valve molar constant (kmol (atm s)^{-1})

K_r – Modelling constant (kmol (s A)^{-1})

M_{H_2} – Molar mass of hydrogen (kg (kmol)^{-1})

n_{H_2} – Number of hydrogen moles in the anode channel (kmol)

N_0 – Number series fuel cells in the stack

N_5 – Number of fuel cell modules

P_{H_2} – Hydrogen partial pressure (atm)

P_{H_2O} – Water partial pressure (atm)

P_{O_2} – Oxygen partial pressure (atm)

q_{O_2} – Input molar flow of hydrogen (kmol (s)^{-1})

$q_{O_2}^{in}$ – Hydrogen input flow (kmol (s)^{-1})

$q_{H_2}^{out}$ – Hydrogen output flow (kmol (s)^{-1})

$q_{H_2}^{req}$ – The amount of hydrogen flow required to meet the load change (kmol(s)^{-1})

R – Universal gas constant ($(1 \text{ atm}) (\text{kmol K})^{-1}$)

R^{in} – FC internal resistance (Ω)

T – Absolute temperature (K)

U – utilization factor

V_{an} – Volume of the anode (m^3)

V_{cell} – DC output voltage of FC system (V)

τ_{H_2} – Hydrogen time constant (s)

τ_{O_2} – Oxygen time constant (s)

τ_{H_2O} – Water time constant (s)

η_{act} – Activation over voltage (V)

η_{ohmic} – Ohmic over voltage (V)

The equation that relates molar flow of any gas (hydrogen) through the valve with its partial pressure in the channel can be expressed as

$$\frac{q_{H_2}}{P_{H_2}} = \frac{K_{an}}{\sqrt{M_{H_2}}} = K_{H_2} \quad (1)$$

The ideal gas equation is applied to hydrogen,

$$P_{H_2} * V_{an} = n_{H_2} * RT \quad (2)$$

From the Eq. (2) Hydrogen pressure can be written as

$$P_{H_2} = \frac{RT}{V_{an}} * n_{H_2} \quad (3)$$

Taking derivatives of the both sides of the above equation give

$$\frac{dP_{H_2}}{dt} = \frac{RT}{V_{an}} * \frac{d}{dt} n_{H_2} = \frac{RT}{V_{an}} * q_{H_2} \quad (4)$$

The derivative of n_{H_2} is q_{H_2} which is hydrogen molar flow. There are three relevant contributions to the hydrogen molar flow; the input flow, the flow taking part in the reaction and output flow. Therefore,

$$\frac{d}{dt} P_{H_2} = \frac{RT}{V_{an}} * (q_{H_2}^{in} - q_{H_2}^{out} - q_{H_2}^r) \quad (5)$$

According to the basic electrochemical relationships, the molar flow of hydrogen that results can be found as

$$q_{H_2}^r = \frac{N_0 I_{FC}}{2F} = 2K_r I_{FC} \quad (6)$$

Where

$$K_r = \frac{N_0}{4F} \quad (7)$$

Inserting Eq. (6) into Eq. (5) results the following equation:

$$\frac{d}{dt} P_{H_2} = \frac{RT}{V_{an}} * (q_{H_2}^{in} - q_{H_2}^{out} - 2K_r I_{FC}) \quad (8)$$

Then, replacing output flow $q_{H_2}^{out}$, by its definition in the Eq. (1) gives:

$$\frac{d}{dt} P_{H_2} = \frac{RT}{V_{an}} * (q_{H_2}^{in} - K_{H_2} P_{H_2} - 2K_r I_{FC}) \quad (9)$$

Taking the Laplace transform of the both sides:

$$sP_{H_2}(s) - P_{H_2}(0) = \frac{RT}{V_{an}} * (q_{H_2}^{in}(s) - K_{H_2}P_{H_2}(s) - 2K_r I_{FC}) \quad (10)$$

Where, the initial condition of hydrogen partial pressure is zero. The following expression gives the hydrogen partial pressure as:

$$P_{H_2} = \frac{\frac{1}{K_{H_2}}}{1 + \tau_{H_2}s} (q_{H_2}^{in} - 2K_r I_{FC}) \quad (11)$$

Where

$$\tau_{H_2} = \frac{V_{an}}{K_{H_2}RT} s \quad (12)$$

Similarly, water partial pressure and oxygen partial pressure can be obtained. The polarization curve for the FC is obtained from the sum of the Nernst's voltage, the activation over voltage, and the ohmic over voltage. Assuming a constant temperature and oxygen concentration, the FC output voltage may be expressed as

$$V_{cell} = E + \eta_{act} + \eta_{ohmic} \quad (13)$$

Where

$$\eta_{act} = -B * \ln(CI_{FC}) \quad (14)$$

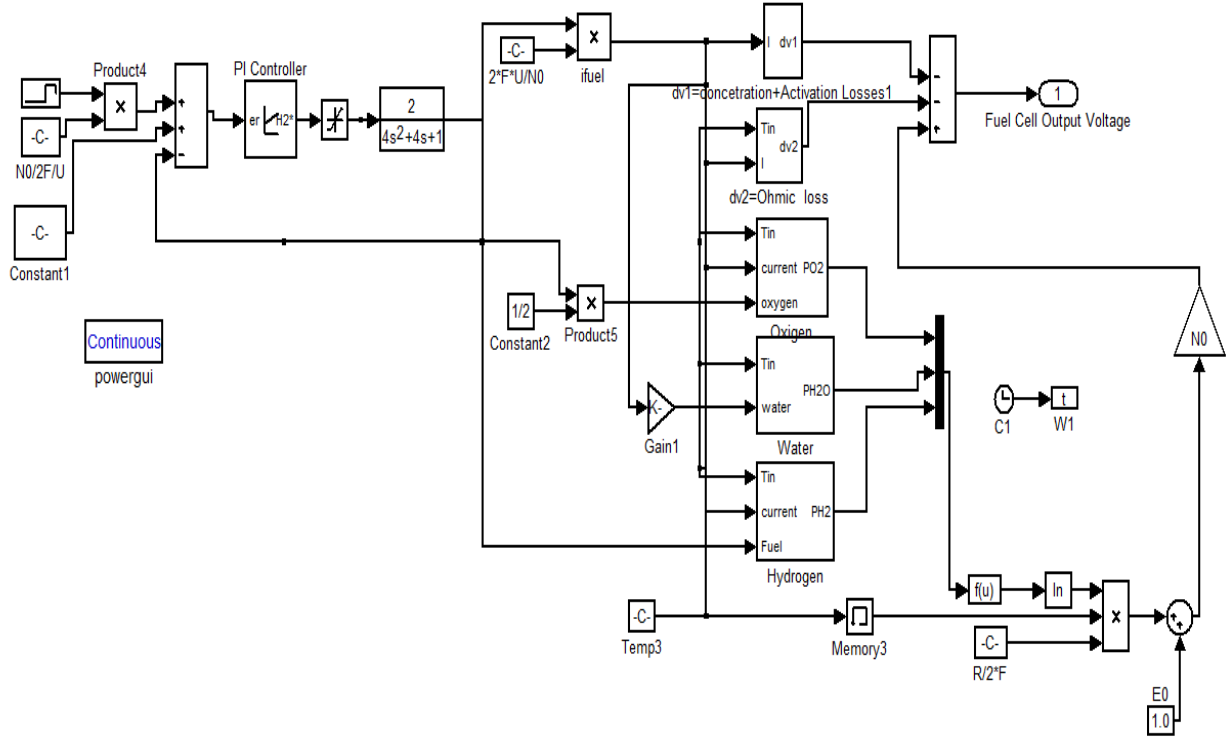


Figure 2.2 Simulink model of fuel cell

and

$$\eta_{ohmic} = -R^{in} * I_{FC} \quad (15)$$

Now, the Nernst's instantaneous voltage may be expressed as

$$E = N_0 \left[E_0 + \frac{RT}{2F} \log \left\{ \frac{P_{H_2} \sqrt{P_{O_2}}}{P_{H_2O}} \right\} \right] \quad (16)$$

The fuel cell system consumes hydrogen according to the power demand. The hydrogen is obtained from a high pressure hydrogen tank for stack operation. During operational conditions, to control the hydrogen flow rate according to the fuel cell power output. The amount of hydrogen available from the hydrogen tank is given by

$$q_{H_2}^{req} = \frac{N_0 I_{FC}}{2FU} \quad (17)$$

Depending on the FC system configuration and the flow of hydrogen and oxygen, the FC system produces the DC output voltage. The hydrogen-oxygen flow ratio r_{H_2O} in the FC system determines the oxygen flow rate.

2.5 Voltage-Current Polarization curve of fuel cell stack

The response of fuel cell that produces electric DC power from hydrogen and oxygen is much faster than that of the reformer. A voltage-current polarization curve of a fuel cell stack represented in fig. 2.3 also needs to be considered in the practical model of the fuel cell. The relation between Cell voltage is inversely proportional to the stack current. The fig. 2.3 shows a static voltage-current characteristic curve of a single cell.

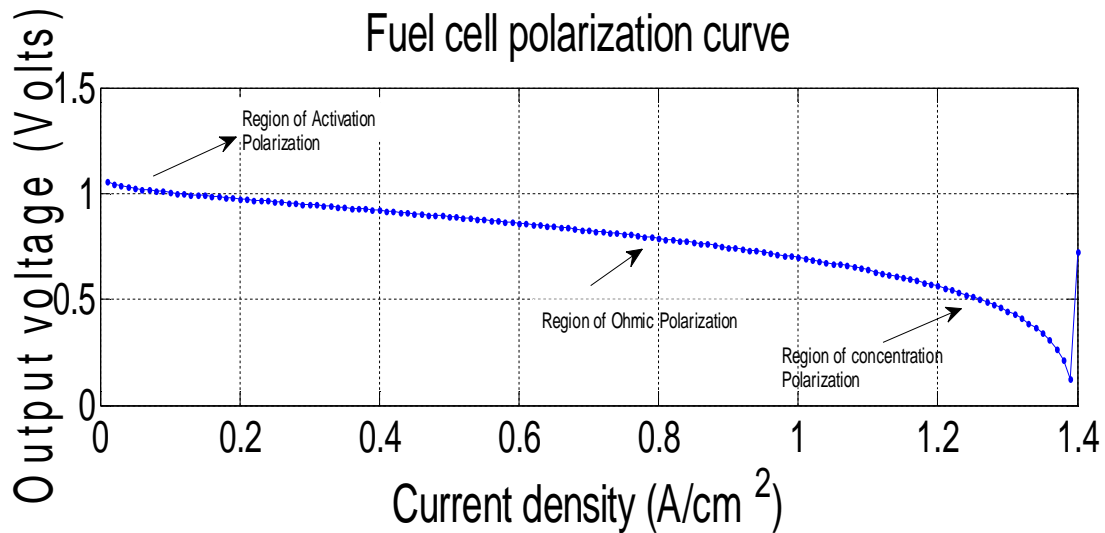


Figure 2.3 Fuel cell polarization curve

As illustrated in the fig. 2.3, there exist three regions, region of activation polarization, region of ohmic polarization, and region of concentration polarization. First, in a region of activation polarization, the cell voltage drops rapidly with even smaller current increase. Second, in the region of ohmic polarization, the cell voltage linearly decreases as current increase. Last,

in region of concentration polarization, the voltage collapses sharply when current exceed the upper limit of safe operation, and as a consequence, operation in this region should be avoided because the fuel cell may be damaged due to primarily starvation of the hydrogen.

2.6 Summary

A PEM Fuel cell is modeled in Simulink. It is best for portable applications such as laptop, mobile etc.; As it operates at low temperature and has high power density with a quick start.

Chapter 3

DC-DC Converter

Chapter 3 : DC-DC CONVERTER

3.1 Introduction

A DC-DC converter is a circuit that converts DC voltage from one voltage level to another or we can say converting the unregulated DC input to a controlled DC output at a desired voltage level. DC-DC converters are now a day's present in all the electronic devices such as laptop, iPad etc. As all the devices have a single power supply battery which is to be converted to a different voltage level of sub-circuits, which simply reduces the space and cost of extra batteries. Fuel cell output voltage shows a sagging characteristic and get affected by the load variation or by changes in supply need. So it is a very necessary part of circuit to enhance the power supply and keep it at a constant level.

This conversion can be done by three different methods and they are

- Linear
- Switched-mode conversion
- Magnetic

Linear conversion can only give output at lower voltages from the input. They cannot be used when the voltage drop is large and the current is high as they dissipate large amounts of heat [7]. Linear regulators are inexpensive, provide a very low-noise output voltage. A popular design approach is to use an LDO, Low Drop-out Regulator. In switching-mode conversion one DC voltage level to another, by storing the input energy temporarily and then releasing that energy to the output of a different voltage; for the storage inductor or capacitor is used. It has increased efficiency. In magnetic method DC-DC converters, energy is periodically stored into and released from a magnetic field in an inductor or a transformer, typically in the range from

300 kHz to 10 MHz [7]. Transformer-based converters may provide isolation between the input and the output.

The functions of dc–dc converters are:

- DC input voltage to a constant DC output voltage.
- To control the dc output voltage against load variations.
- To reduce the ac voltage ripple on the dc output voltage.
- To provide isolation between the input the load.

The dc-dc converters further can be divided into two main types: hard-switching PWM converters, and resonant or soft-switching converters. The PWM converters have been very popular and widely used at every power levels [8]. Advantages of PWM converters include low component count, high efficiency, constant frequency operation, relatively simple control and commercial availability of integrated circuit controllers, and ability to achieve high conversion ratios for both step-down and step-up application. A disadvantage of PWM dc-dc converters is losses in semiconductor devices which limit practical operating frequencies.

3.2 Types of DC-DC converter

The dc-dc converters which are mostly used in switch-mode dc power supplies are:

1. Step-down (buck) converter
2. Step-up (boost) converter
3. Step-down/step-up (buck- boost) converter
4. Cuk converter
5. Full-bridge converter

The step-down and the step-up are the basic converter topologies. The buck-boost and the Cuk converters are combinations of above two topologies. The full-bridge converter is derived from the step-down converter.

3.2.1 Step-down (buck) converter:

A buck converter is a step-down DC to DC converter. Its design is similar to the step-up boost converter, and like the boost converter it is a switched-mode power supply that uses two switches (a transistor and a diode), an inductor and a capacitor.

The step-down dc–dc converter, commonly known as a buck converter consists of a dc input voltage source, controlled switch, diode, filter inductor, filter capacitor, and load resistance. There are two mode of operation which is made on the basis of inductor current. When inductor current is never zero for any period of time is called the continuous conduction mode (CCM), and other is Discontinuous conduction mode (DCM).

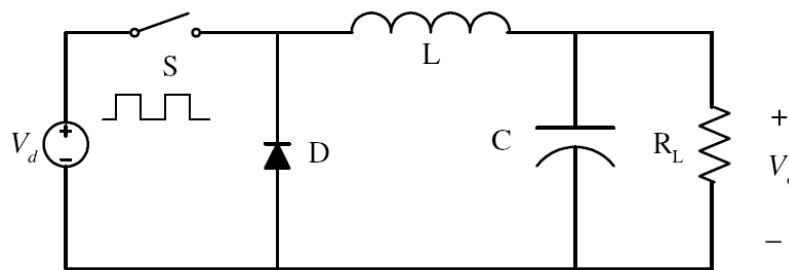


Figure 3.1 Buck converter circuit diagram

3.2.1.1 Working of Buck converter

The circuit operates in two conditions; when the switch is closed and other when it is open. The switch is operated by a switching pulse. At the high pulse or when the switch is on/closed diode is reversed biased and conducts inductor current in forward direction. During

this period a positive voltage will appear across inductor. And inductor current will increase gradually. Output voltage and current during this period will be

$$V_L = V_d - V_o \quad (1)$$

$$i_L = \frac{1}{L} \int V_L dt \quad (2)$$

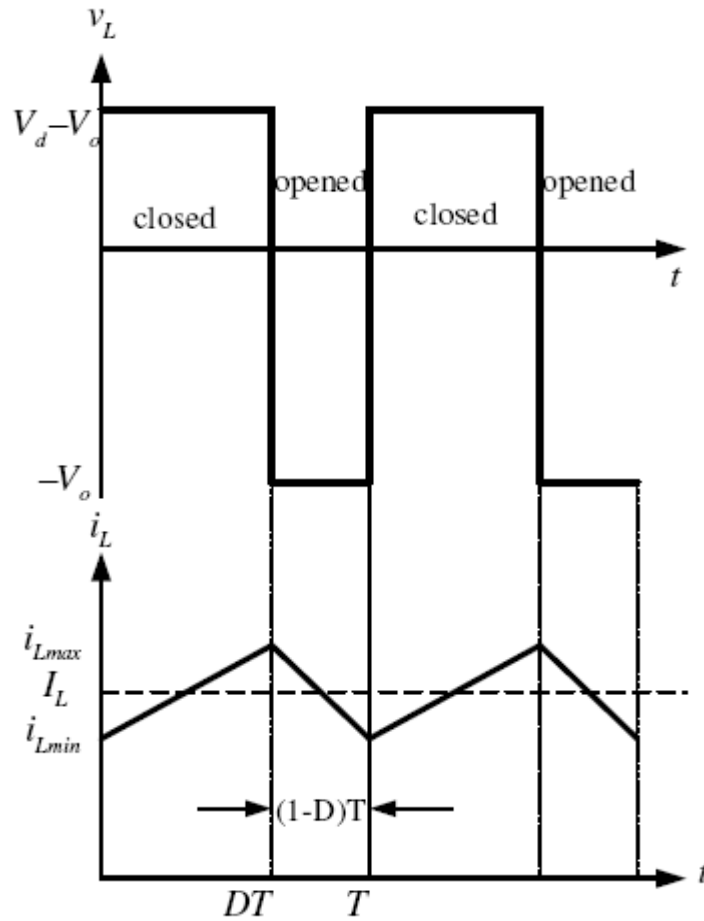


Figure 3.2 Inductor Current of buck converter during On and Off period

We can derive the change in inductor current as.

$$V_L = V_d - V_o = L \frac{di_L}{dt} \quad (3)$$

$$\frac{di_L}{dt} = \frac{V_d - V_o}{L} \quad (4)$$

Assuming the ideal condition the inductor current will increase linearly as shown in figure 3.2

So change in inductor current by time duration can be written as

$$\frac{di_L}{dt} = \frac{\Delta i_L}{\Delta t} = \frac{\Delta i_L}{DT} \quad (5)$$

From equation (4) and (5)

$$\Delta i_L = \frac{V_d - V_o}{L} \cdot DT \quad (6)$$

Now when the switch will be open diode will be forward biased and will act as short circuited. Now the current flow will take place through diode. The stored inductor energy will give i_L continues to flow. The voltage across inductor will be

$$V_L = -V_o \quad (7)$$

$$V_L = -V_o = L \frac{di_L}{dt} \quad (8)$$

$$\frac{di_L}{dt} = \frac{-V_o}{L} = \frac{\Delta i_L}{\Delta t} = \frac{\Delta i_L}{(1-D)T} \quad (9)$$

$$\Delta i_L = \frac{-V_o}{L} \cdot (1-D)T \quad (10)$$

For a steady state operation change in inductor current should be zero over a period. Therefore sum of the equation (6) and (10) it should be zero.

$$\frac{V_d - V_o}{L} \cdot DT + \frac{-V_o}{L} \cdot (1-D)T = 0 \quad (11)$$

This reduces to

$$V_o = DV_d \quad (12)$$

From equation (12) plot will be

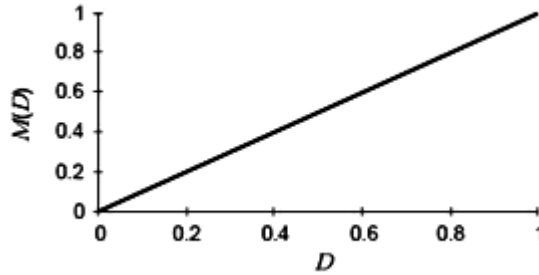


Figure 3.3 Plot of gain verses duty cycle

3.2.1.2 Analysis of Buck converter

From equation (12), we can say that output voltage is depends on the duty cycle which can vary from zero to unity. So, it is called Step-down (Buck) converter. There are two mode of operation one is Continuous Current mode (CCM) and the second is Discontinuous Current mode (DCM). Buck converter to operate in CCM the parameters should be as given below:

Inductor value should

$$L > L_{min} = \frac{(1 - D)}{2f} * R \quad (13)$$

Capacitor value is decided by the output voltage ripples desired

$$C = \frac{(1 - D)}{8Lf^2r} \quad (14)$$

$$r = \frac{\Delta V_o}{V_o} \quad (15)$$

3.2.2 Step-up (boost) converter:

A boost converter is a DC to DC power converter with an output voltage greater than its input voltage. It is a class of switched-mode power supply (SMPS) containing at least two semiconductor switches (a diode and a transistor) and at-least one energy storage element, a capacitor, inductor, or the two in combination. Filters are used to reduce the output voltage ripple. Fig 3.4 shows the circuit diagram of a boost converter.

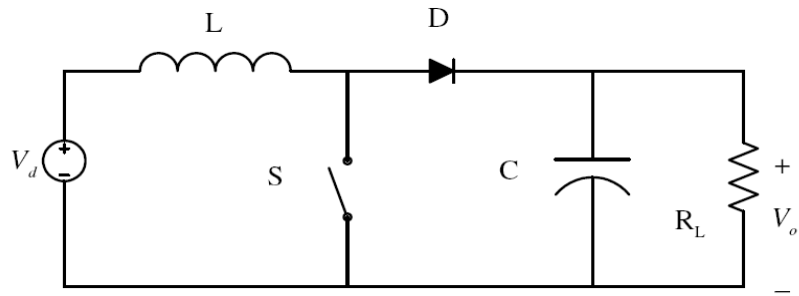


Figure 3.4 Boost converter circuit diagram

3.2.2.1 Working of the boost converter

The energy is transferred from input voltage source to output load. The output voltage is higher than the input voltage. There is a switch which is closed then the inductor will get energized and store the energy during on time period of the switching signal, and diode will be open circuited. So output circuit will be disconnected.

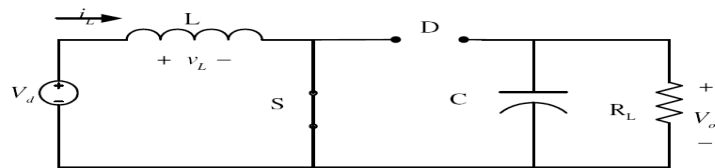


Figure 3.5 Boost converter during ON period of switching pulse

When the switch is open diode will forward biased and the current will flow in load. Current will be summation of the supply current and stored in inductor during the on period of switching signal.

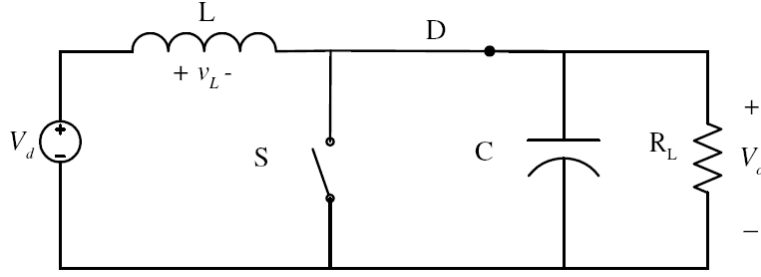


Figure 3.6 Boost converter during OFF period of switching pulse

During the on period when switch is close inductor current will increase linearly, and the voltage across the inductor will be

$$V_L = V_d = L \frac{di_L}{dt} \quad (16)$$

$$\frac{di_L}{dt} = \frac{\Delta i_L}{\Delta t} = \frac{\Delta i_L}{DT} \quad (17)$$

Therefore, the change in inductor current during on period will be

$$(\Delta i_L)_{close} = \frac{V_d DT}{L} \quad (18)$$

When the switch will be open voltage across inductor will be the difference of source voltage and the output voltage

$$V_L = V_d - V_o = L \frac{di_L}{dt} \quad (19)$$

So,

$$\frac{di_L}{dt} = \frac{V_d - V_o}{L} \quad (20)$$

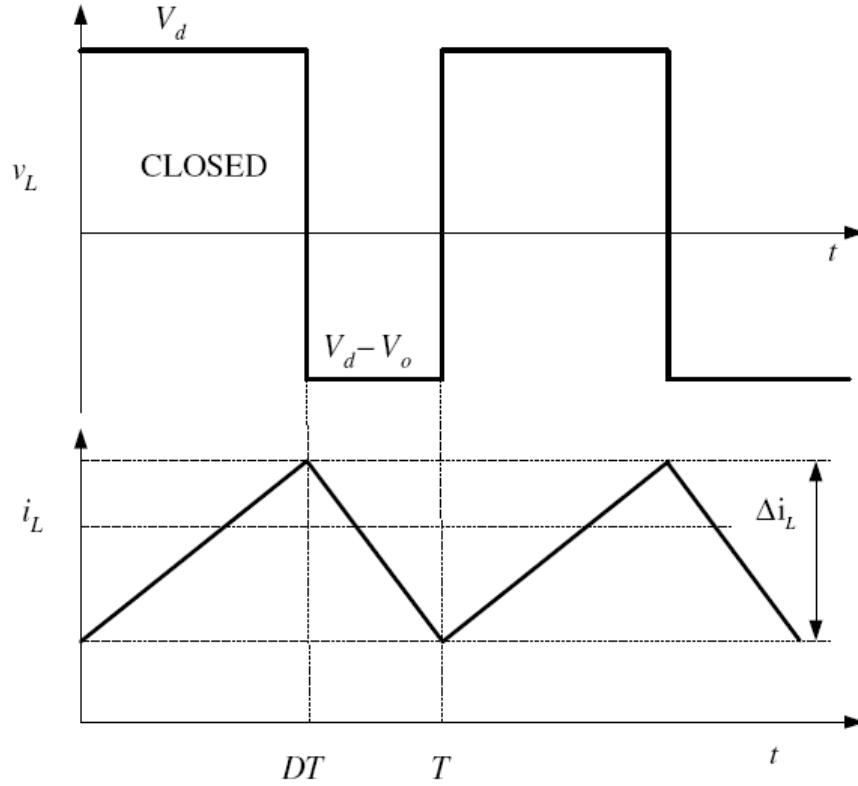


Figure 3.7 Inductor current of Boost converter

We can also write

$$\frac{di_L}{dt} = \frac{\Delta i_L}{\Delta t} = \frac{\Delta i_L}{(1-D)T} \quad (21)$$

Change in inductor current during off period

$$(\Delta i_L)_{open} = \frac{(V_d - V_o)(1-D)T}{L} \quad (22)$$

Boost converter to work in a steady-state condition the change in inductor current during one period of time must be zero.

$$(\Delta i_L)_{close} + (\Delta i_L)_{open} = 0 \quad (23)$$

This reduces to

$$V_o = \frac{V_d}{(1 - D)} \quad (24)$$

From above equation, we can say Boost converter produces output voltage that is greater or equal to the input voltage. Plotting a graph between the output voltage and duty cycle

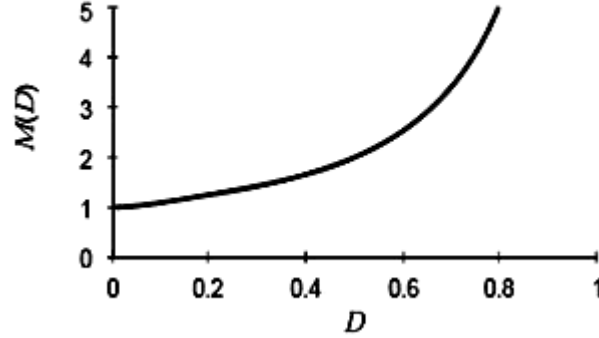


Figure 3.8 Plot of gain verses duty cyle of boost converter

3.2.2.2 Analysis of Boost converter

Boost converter operates in two mode one is Continuous Current mode (CCM) and the second is Discontinuous Current mode (DCM). Boost converter to operate in CCM the parameters should be as given below:

For CCM

$$I_{min} \geq 0 \quad (25)$$

Where

$$I_{min} = \frac{V_d}{(1 - D)^2 R} - \frac{V_d D T}{2L} \quad (26)$$

We deduce minimum value of inductor

$$L_{min} = \frac{D(1 - D)^2 R}{2f} \quad (27)$$

Capacitor value

$$C = \frac{D}{Rfr} \quad (28)$$

$$r = \frac{\Delta V_o}{V_o} \quad (29)$$

3.2.3 Buck-Boost converter:

The main application of a buck-boost converter is in regulating dc power. The output voltage can be either higher or lower than the input voltage. A buck-boost converter can be obtained by the cascade connection of the two basic converters: the step-down converter and the step-up converter. When the switch is closed, the input provides energy to the inductor and the diode is open. When the switch is open, the energy stored in the inductor is transferred to the output. No energy is supplied by the input during this interval.

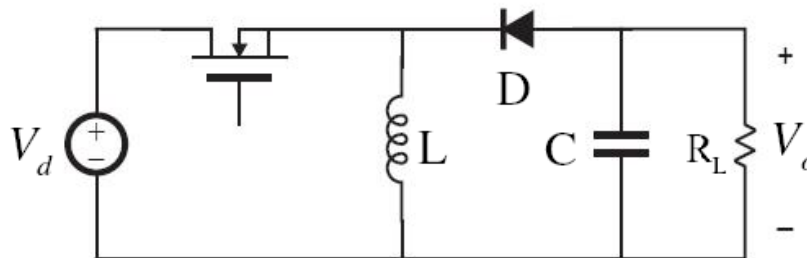


Figure 3.9 Buck-boost converter circuit diagram

3.2.3.1 Working of the Buck-boost converter

Buck-boost converter stores the energy during the on period of switching pulse and when switch is open during off period of switching pulse it supply all the energy to output.

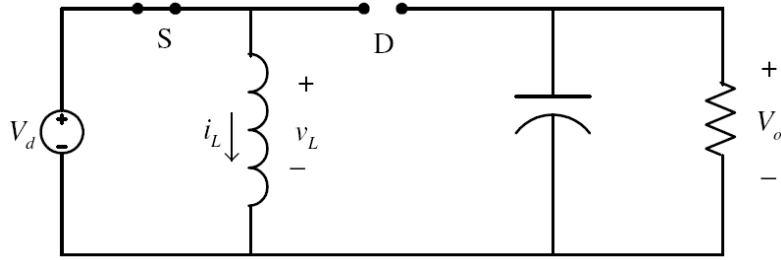


Figure 3.10 Buck-boost converter when switch closed

When switch is close voltage across inductor is equal to supply voltage and the diode is reverse biased.

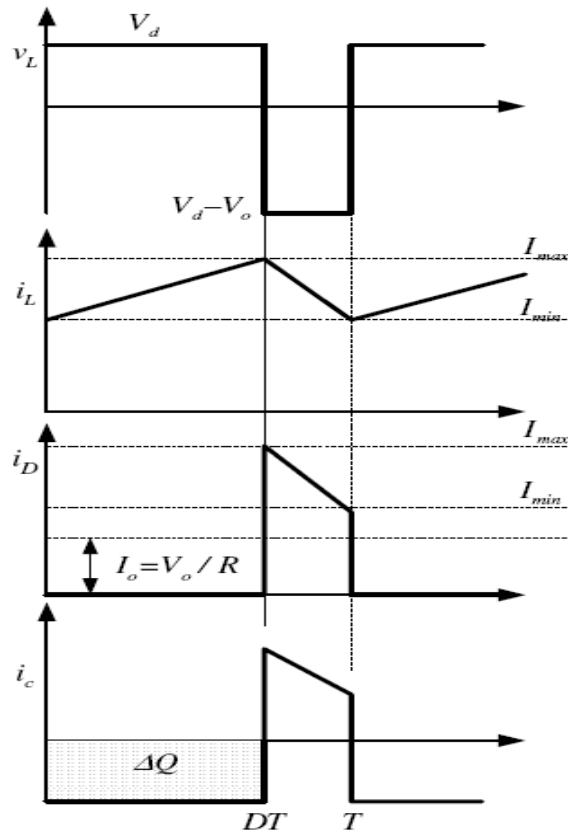


Figure 3.11 Inductor current of buck-boost converter

$$V_L = V_d = L \frac{di_L}{dt} \quad (30)$$

$$\frac{di_L}{dt} = \frac{V_d}{L} \quad (31)$$

Change in inductor current during on time

$$(\Delta i_L)_{close} = \frac{V_d DT}{L} \quad (32)$$

When switch is opened inductor voltage across it

$$V_L = V_O = L \frac{di_L}{dt} \quad (33)$$

$$\frac{di_L}{dt} = \frac{V_O}{L} \quad (34)$$

Change in inductor current

$$(\Delta i_L)_{open} = \frac{V_d(1-D)T}{L} \quad (35)$$

For steady-state operation total current change during one complete period must be zero

$$(\Delta i_L)_{close} + (\Delta i_L)_{open} = 0 \quad (36)$$

$$V_O = -V_d \frac{D}{(1-D)} \quad (37)$$

Output of a buck-boost converter either be higher or lower than input depends on duty cycle which as

- If $D > 0.5$, output is higher than input
- If $D < 0.5$, output is lower input

Output voltage is always negative. Output is never directly connected to load. Energy is stored in inductor when switch is closed and transferred to load when switch is opened.

3.3 Simulation

MATLAB/SIMULINK simulated models of DC-DC converters fuel cell as the input voltage source and the output waveform of current and voltage.

BUCK Converter

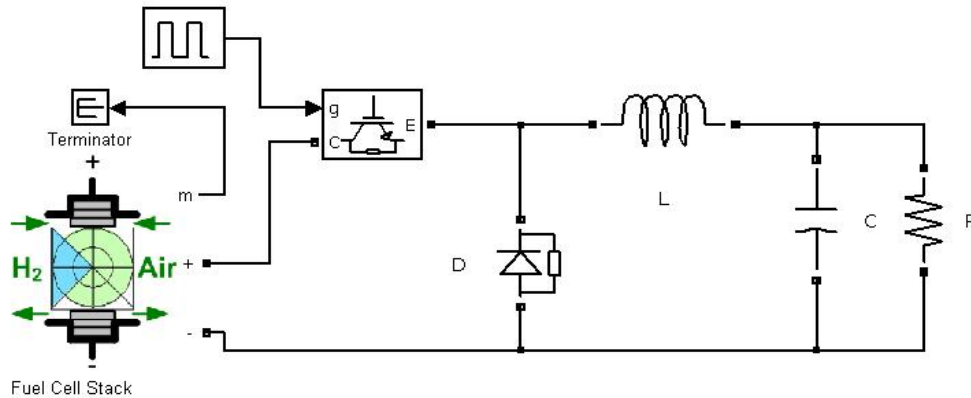


Figure 3.12 Simulink model buck converter

Output waveform of buck converter

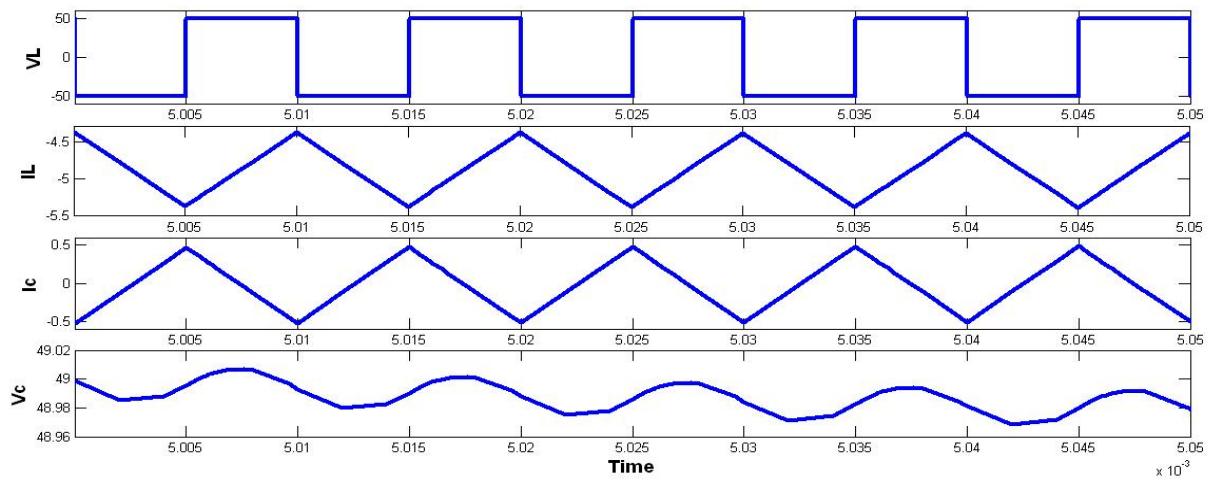


Figure 3.13 Output waveform of buck converter

BOOST Converter

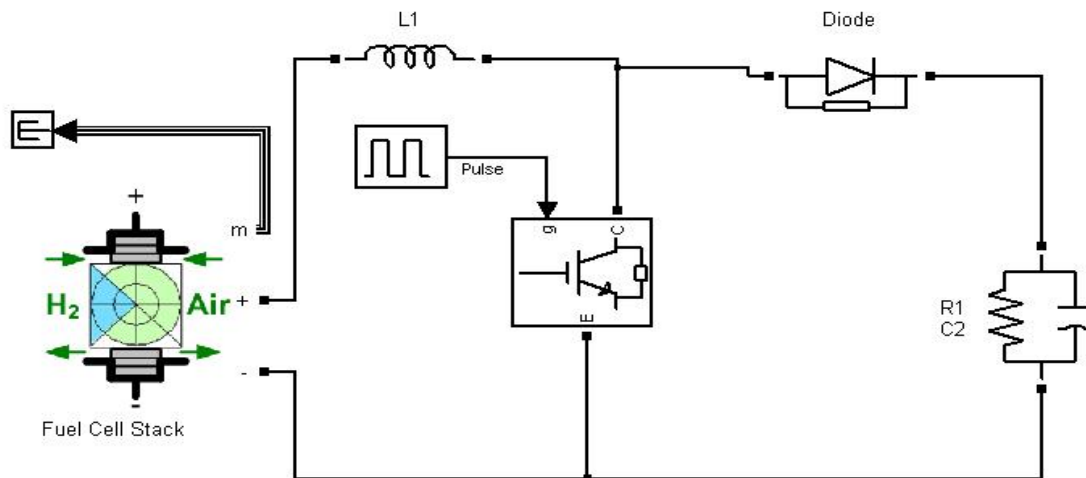


Figure 3.14 Simulink model of boost converter

Output waveform of boost waveform

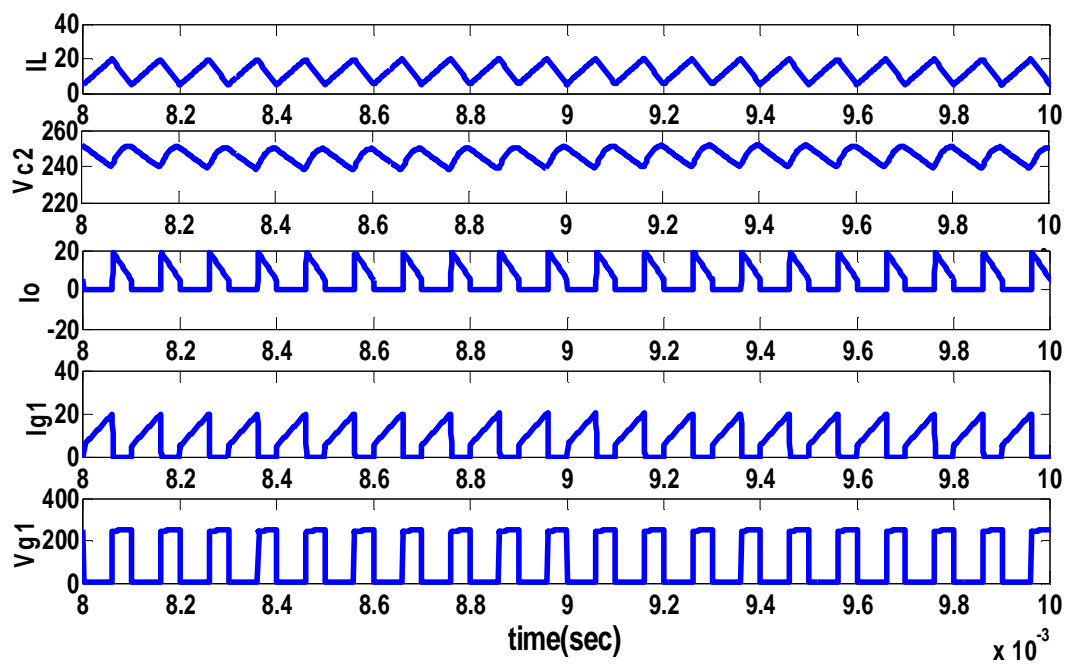


Figure 3.15 Output waveform of boost converter

BUCK-BOOST Converter

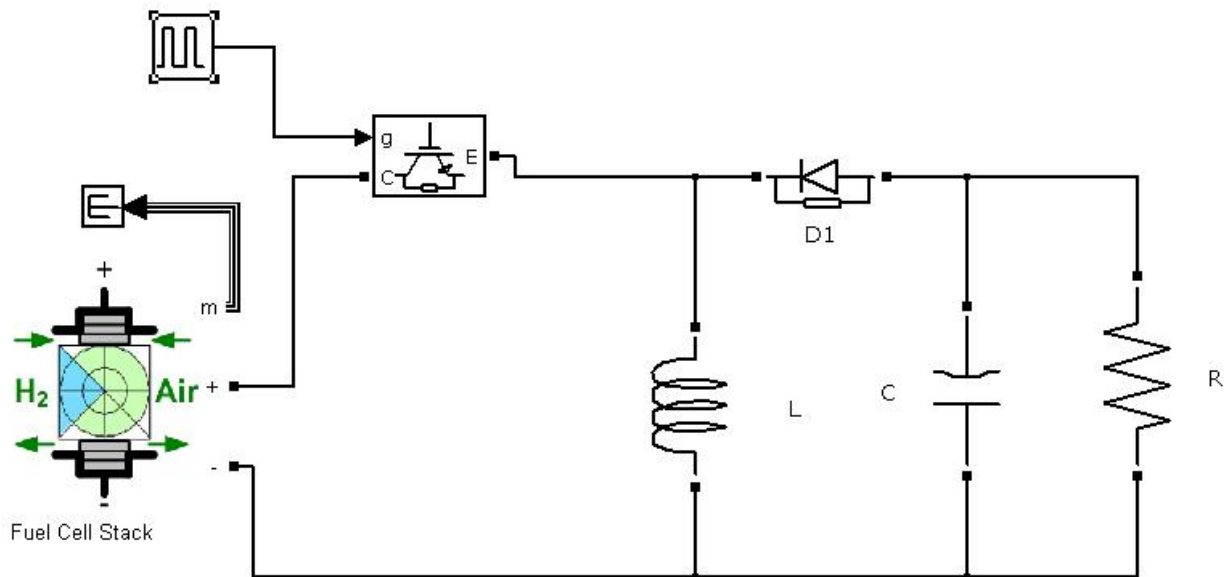


Figure 3.16 Simulink model of buck-boost converter

Output waveform of BUCK-BOOST converter

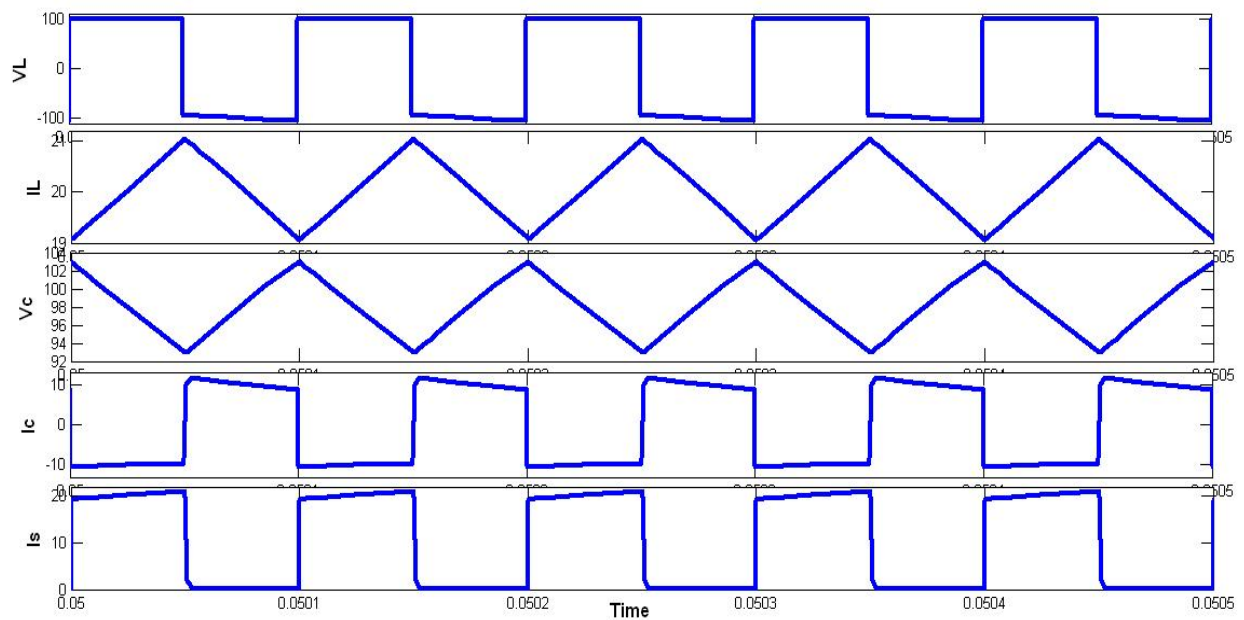


Figure 3.17 Output waveform of buck-boost converter

3.4 Summary

Different types of DC-DC converter are simulated in MATLAB/SIMULINK. The Boost converter has the highest efficiency as it gives output voltage greater than the input, but when it is desired to have a lower output voltage during low power need it fails and similarly the Buck converter. So the Buck-Boost converter topology is used which can give both the higher and lower output voltage. It was seen we need a low resistance in series with the inductor to get same voltage swing as we got in simulation. The values of component which are taken $L=8\text{ mH}$, $C=100\text{ }\mu\text{F}$, $R(\text{series with inductor})=20\text{ }\Omega$ and load resistance $10\text{ }\Omega$.

Chapter 4

Control Strategy

Chapter 4 : CONTROL STRATEGY

4.1 Introduction

In dc-dc converters, the average dc output voltage must be controlled to equal a desired level, though the input voltage and the output load may fluctuate. Switch-mode dc-dc converters utilize one or more switches to transform dc from one level to another. In a dc-dc converter with a given input voltage, the average output voltage is controlled by controlling the switch on and off durations [9]. To illustrate the switch-mode conversion concept, consider a basic dc-dc converter. The average value of the output voltage depends on t_{on} and t_{off} .

There are two methods for controlling the output voltage one by switching at a constant frequency (hence, a constant switching time period ($T_s = t_{on} + t_{off}$)) and adjusting the on duration of the switch to control the average output voltage. In this method, called pulse-width modulation (PWM) switching, the switch duty ratio D , which is defined as the ratio of the on duration to the switching time period, is varied. The other control method is more general, where both the switching frequency (and hence the time period) and the on duration of the switch are varied. Variation in the switching frequency makes it difficult to filter the ripple components in the input and the output waveforms of the converter.

4.2 PWM (Pulse Width Modulation) scheme

In the PWM switching at a constant switching frequency, the switch control signal, which controls the state (on or off) of the switch, is generated by comparing a signal-level control voltage, with a repetitive waveform [10].

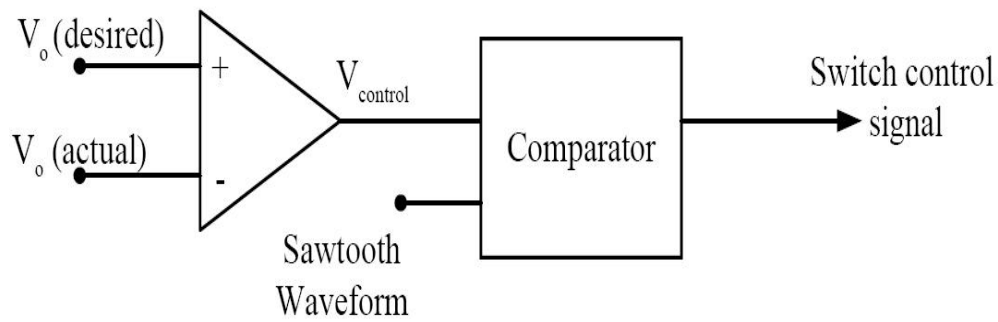


Figure 4.1 Block diagram PWM signal generation

The control voltage signal generally is obtained by amplifying the error, or the difference between the actual output voltage and its desired value. The frequency of the repetitive waveform with a constant peak, which is shown to be a saw-tooth, establishes the switching frequency. This frequency is kept constant in a PWM control and is chosen to be in a few kilohertz to a few hundred kilohertz range [10]. When the amplified error signal, which varies very slowly with time relative to the switching frequency, is greater than the saw-tooth waveform, the switch control signal becomes high, causing the switch to turn on. Otherwise, the switch is off.

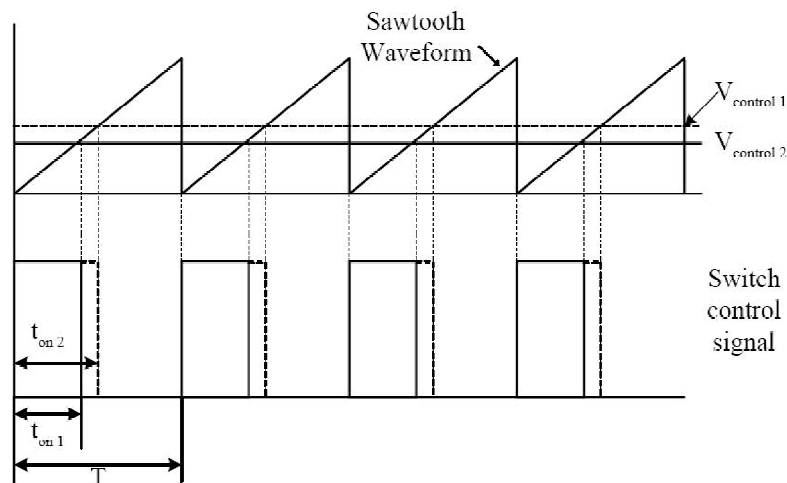


Figure 4.2 PWM Duty cycle control diagram

4.2.1 FPGA Implementation of PWM

PWM signal is generated in VHDL. A repetitive signal is generated by a counter, which count from zero to maximum and when it reaches the maximum count the counter is reset to zero again. This process is repeated concurrently in a process block. The frequency of the PWM signal is decided by the frequency of this repetitive signal. The N-bit comparator is used, which compares the counter count and the N-bit input which is from the PI controller. When the input is high it will generate a high signal and when the input is lower than a low signal is generated. In this way the PWM signal is generated which drives the power switch of the converter.



Figure 4.3 Entity of PWM

A 24 bit input is taken which is compared with a 24 bit counter. The global clock which is available in SPARTAN 3E board is of 50 MHz frequency [13]. The minimum frequency of PWM signal can be generated is 3 Hz. To get a frequency of our desired we need to count more at a time.

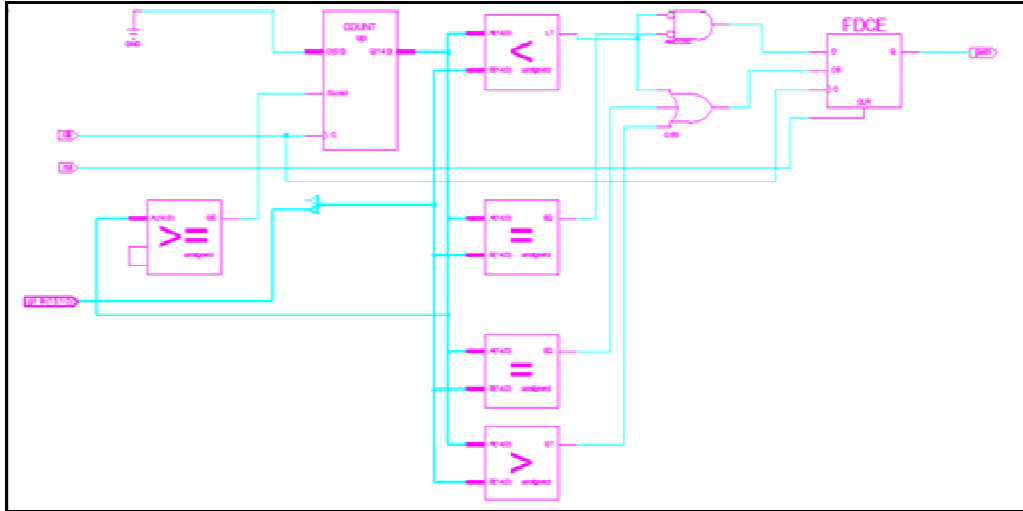


Figure 4.4 RTL schematic of PWM

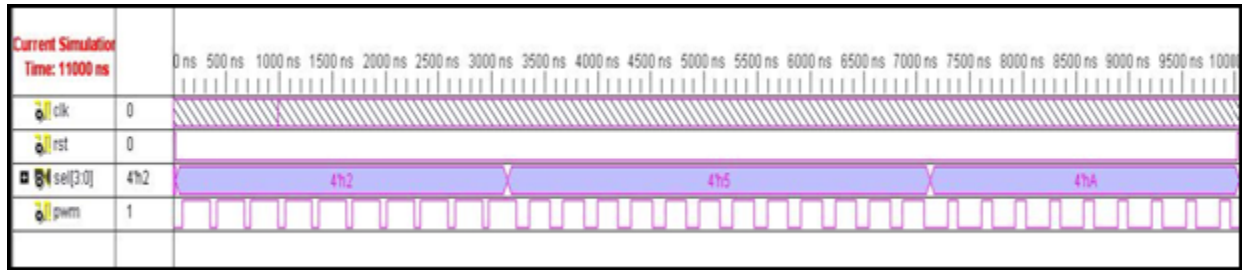


Figure 4.5 Test bench waveform of PWM

4.2.2 Design summary

Table 4.1 Design summary of PWM

Logic Utilization	Used	Available	Utilization
No. of slice flip flops	16	9312	1%
No. of 4 input LUTs	26	9312	1%
No. of Occupied Slices	16	4656	1%
No. of slices containing only related logic	16	16	100%
Total no. of 4 input LUTs	27	9312	1%
No. of bonded IOBs	3	232	1%

4.4 Proportional Integral Control

Proportional-Integral (PI) compensator is used to guarantee null steady-state error with acceptable rise times. The PI compensator is a particular case of lag-lead compensator, therefore suitable for converters with good stability margin but poor steady-state accuracy. The PI feedback control method adds positive corrections, removing the error from a system's controllable variable. PI control method consists of two actions, the proportional action and the integral action. The proportional action involves multiplying the error with a constant (Proportional gain) and adding the product to the controlled quantity. The principle of proportional action requires that the amount of change in the manipulated variable vary directly with the size of the error that is the proportional gain dictates the sensitivity of the correction action. The integral action involves integrating the error over a period of time and then multiplies with a constant (Integral gain) and adding the product to the controlled quantity. Therefore, this action averages the measured error over a period of time to find the process average output error from the desired value. Integral action brings the controlled variable back to the set point in the presence of a sustained upset or disturbance that is integral action acts to eliminate steady state error [8].

The PI controller output which is summation of a proportional term and an integral term can be written as:

$$PI_{out} = K_P * \Delta + K_I \int \Delta dt \quad (1)$$

Where, K_p is proportional gain, K_I is integral gain and Δ is the error input.

4.4.1 FPGA Implementation of PI controller

Implementation of PI controller in FPGA using VHDL we need to convert the equation (1) into a discrete form as the realization of anything in FPGA must be in digital. Equation (1) is converted to discrete form using the numerical method approach [14]. Simplifying the integral term using Trapezoidal method which where it can be written as:

$$\frac{1}{s} \Rightarrow \frac{T}{2} \frac{(Z + 1)}{(Z - 1)} \quad (2)$$

Integral part can be written as:

$$y(n) = x(n) + K_I * \frac{T}{2} * u(n) \quad (3)$$

$$x(n) = y(n) + K_I * \frac{T}{2} * u(n) \quad (4)$$

Where $y(n)$ is output, $u(n)$ is error input, $x(n)$ is the state. And K_I is the integral gain.

The complete PI controller equation which has been implemented is:

$$y(n) = y(n - 1) + K_P * u(n) + K_I * \frac{T}{2} * [u(n - 1) + u(n)] \quad (5)$$

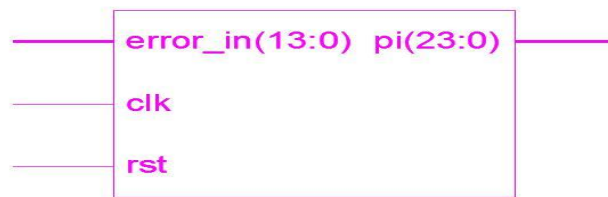


Figure 4.6 Entity of PI controller

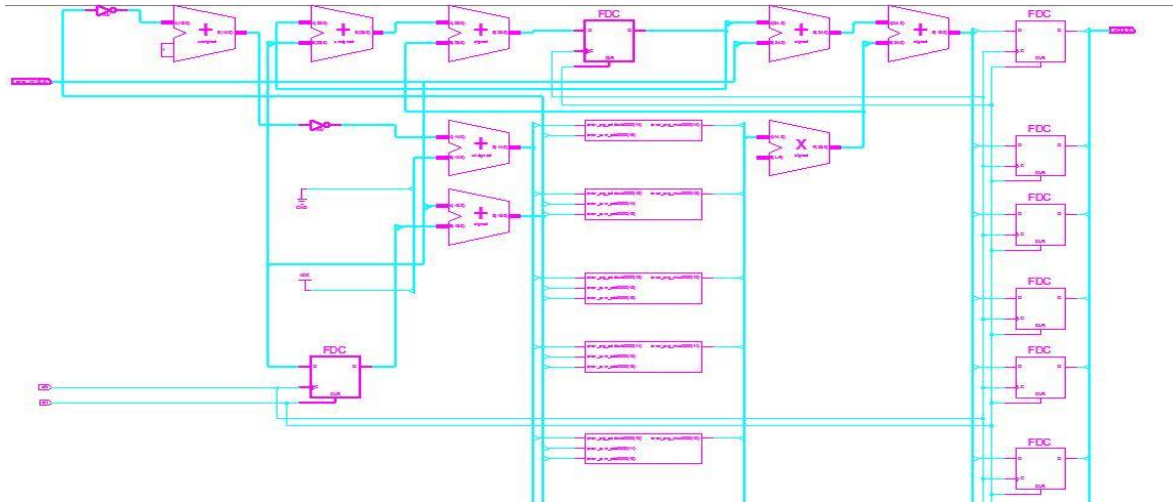


Figure 4.7 RTL schematic of PI controller

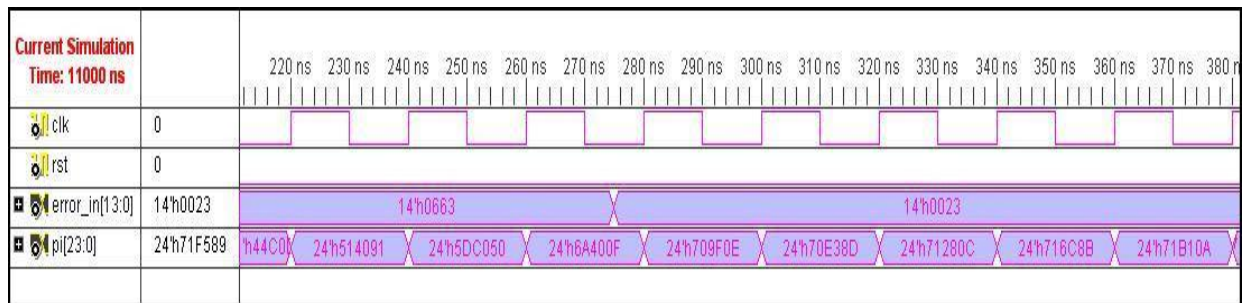
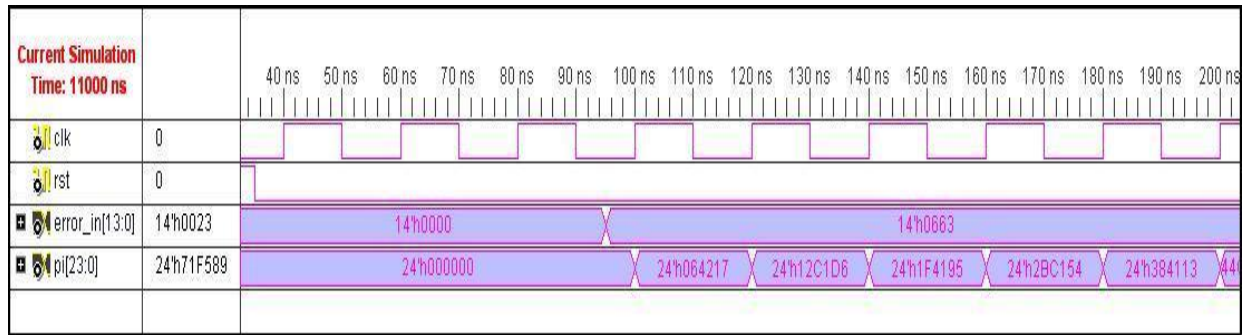


Figure 4.8 Test bench waveform of PI controller

4.4.2 Design summary

Table 4.2 (Design summary of PI controller)

Logic Utilization	Used	Available	Utilization
No. of slices	76	4656	1%
No. of slice flip flop	48	9312	0%
No. of 4 input LUTs	139	9312	1%
No. of bonded IOBs	40	232	17%
No. of GCLKs	1	24	4%

4.5 FPGA implementation of PI and PWM

Control strategy as discussed in previous chapter is needed to be interfaced with the error signal generated from the output voltage and the desired voltage reference. As this signal is an analog signal which is to be converted to a digital representation, for this purpose we need ADC. In Spartan 3E board ADC is available with a programmable pre-amplifier which are Linear Technology LTC6912-1 and Linear Technology LTC1407A-1 respectively. Both the pre-amplifier and the ADC are serially programmed or controlled by the FPGA.[13].

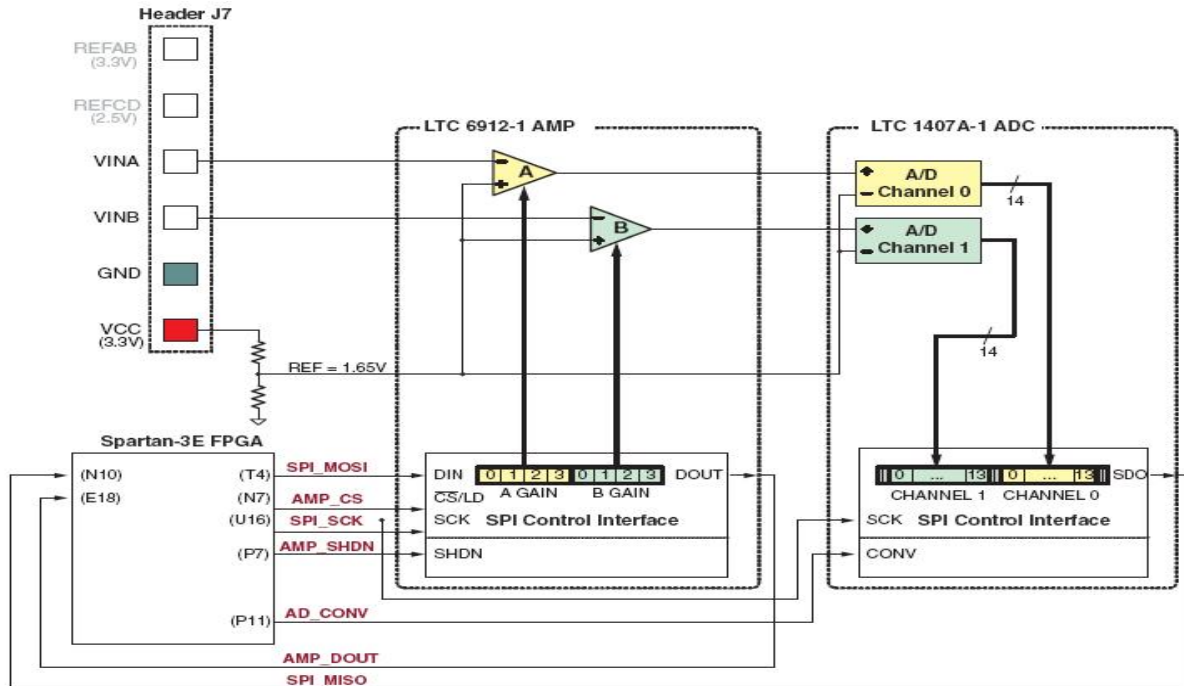


Figure 4.9. Analog capture circuit in Spartan 3E board [13]

The GAIN setting has to be loaded into the programmable pre-amplifier. The various allowable settings of GAINS are Table 4.1. The maximum range of the ADC input is $\pm 1.25V$, centered around 1.65V. The ADC presents a 14-bit, two's complement digital output.

Table 4.4.3 (Programmable Gain of Pre-amplifier)[13]

Gain	A3	A2	A1	A0	Input Voltage Range	
	B3	B2	B1	B0	Minimum	Maximum
0	0	0	0	0	--	--
-1	0	0	0	1	0.4	2.9
-2	0	0	1	0	1.025	2.275
-5	0	0	1	1	1.4	1.9
-10	0	1	0	0	1.525	1.775
-20	0	1	0	1	1.5875	1.7125
-50	0	1	1	0	1.625	1.675
-100	0	1	1	1	1.6375	1.6625

4.5.1 SPI interface signals of Amplifier to FPGA

First we need to get the gain of the pre-amplifier and then we can take sample from the input pin of ADC. To configure the amplifier which communicates serially with the FPGA gain value is send serial. The serial interface signals are:

Table 4.4 (SPI interface signals)

Signal	FPGA Pin	Direction	Description
SPI_MOSI	T4	FPGA=>AD	Serial data: Master Output, Slave Input.
AMP_CS	N7	FPGA=>AMP	Active-Low chip-select.
SPI_SCK	U16	FPGA=> AMP	Clock
AMP_SHDN	P7	FPGA=> AMP	Active-High shutdown, reset
AMP_DOUT	E18	FPGA<= AMP	Serial data, Echoes previous AMP gain.

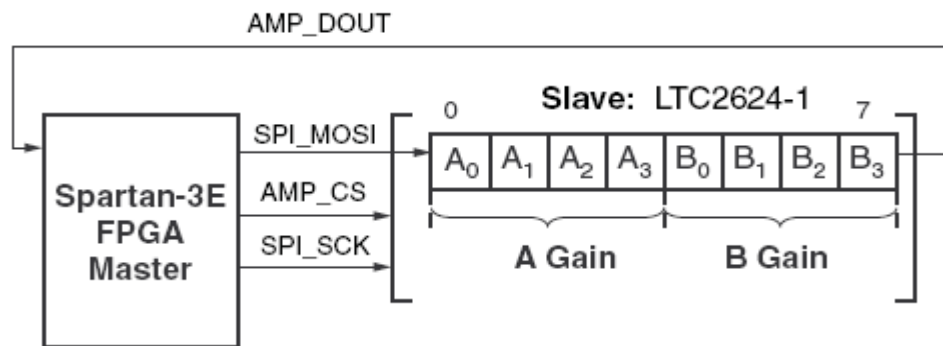


Figure 4.10 SPI signal interface to amplifier

Timing diagram for configuring amplifier, which gives the minimum set-up and hold time for any signal.

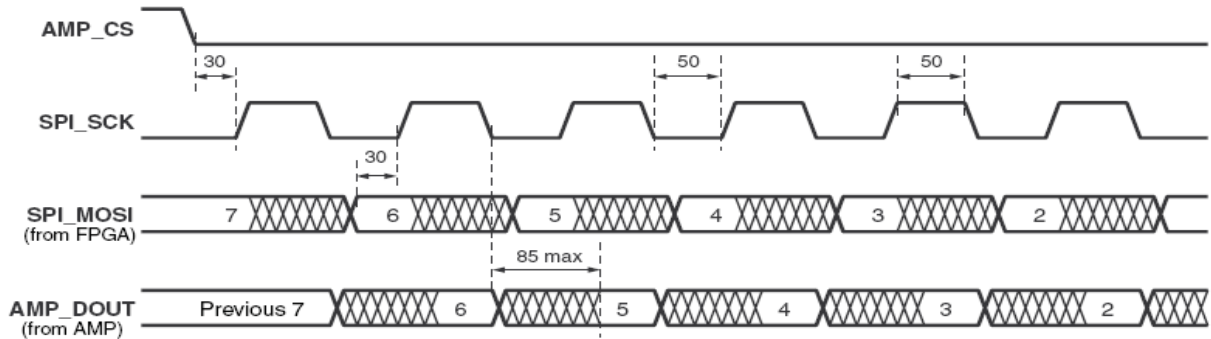


Figure 4.11 Timing diagram of amplifier[13]

The amplifier interface is relatively slow, supporting only about a 10 MHz clock frequency.

4.5.2 State diagram to configure Amplifier gain

FSM is written to configure the amplifier. Moore finite state machine is used where output depends on only the state not on the input. When the AMP_CS signal get low on next SPI_SCK rising edge the data is send to amplifier but the data must be set-up 30 ns before the rising edge.

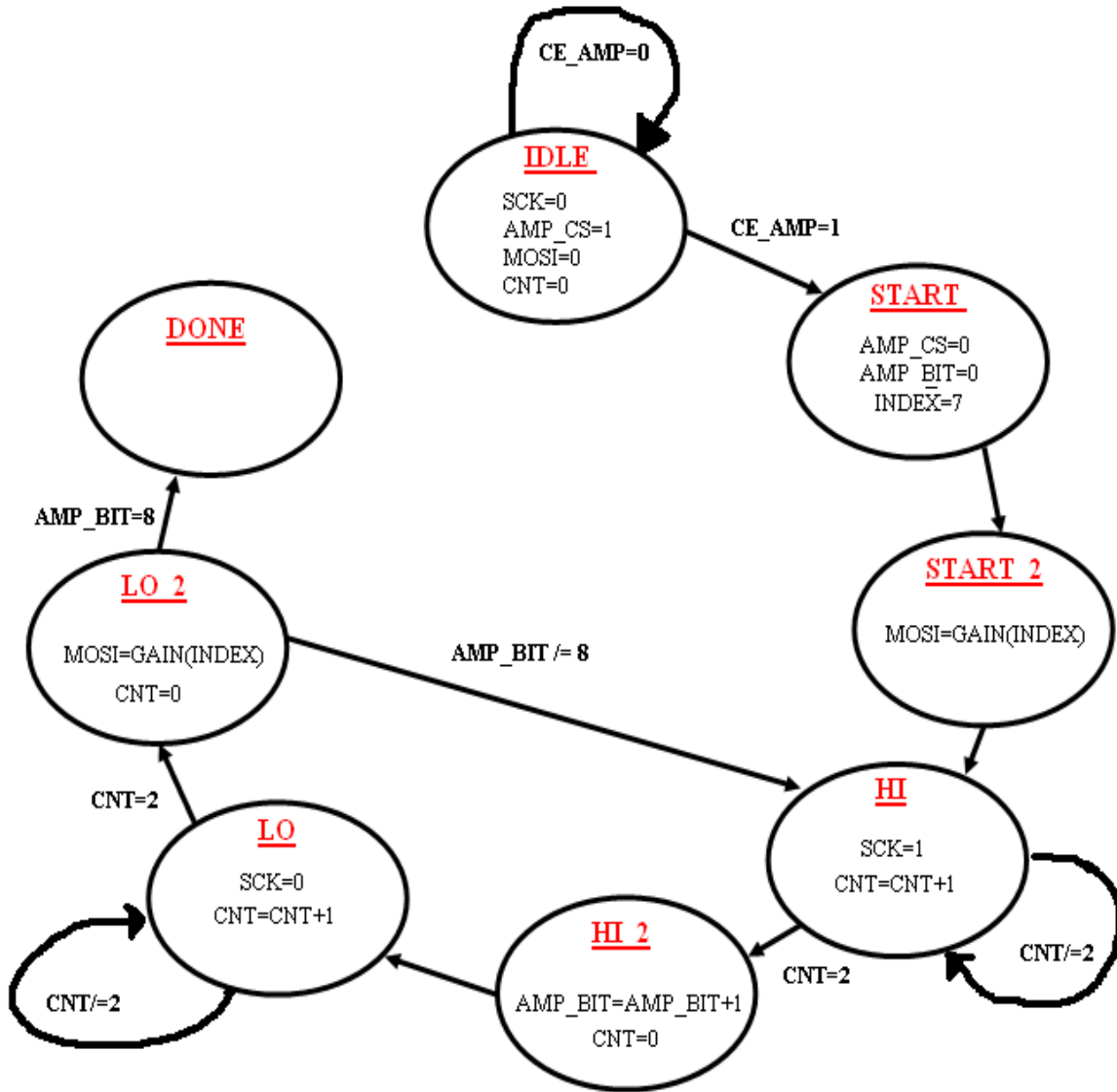


Figure 4.12 FSM for setting gain of amplifier

4.5.3 SPI interface signals of ADC

When the AD_CONV signal goes high, the ADC simultaneously samples both analog channels. The results of this conversion are not presented until the next time AD_CONV is asserted, a latency of one sample. The maxim sample rate is approximately 1.5 MHz The ADC presents the digital representation of the sampled analog values as a 14-bit, two's complement binary value. The AD_CONV signal is not a traditional SPI slave select enable. Be sure to

provide enough SPI_SCK clock cycles so that the ADC leaves the SPI_MISO signal in the high-impedance state. Otherwise, the ADC blocks communication to the other SPI peripherals. As shown in Figure 10-6, use a 34-cycle communications sequence. The ADC 3-states its data output for two clock cycles before and after each 14-bit data transfer [13].

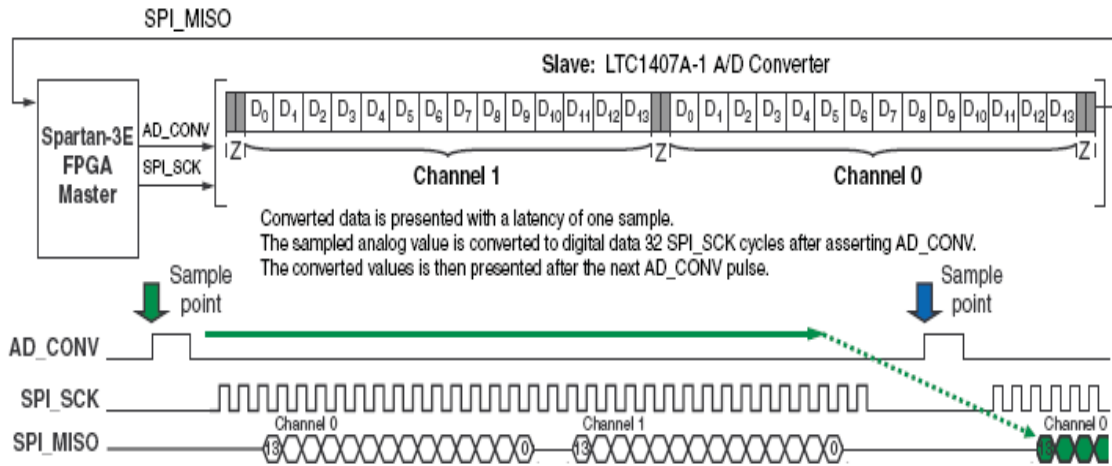


Figure 4.13 SPI signal interface of ADC [13]

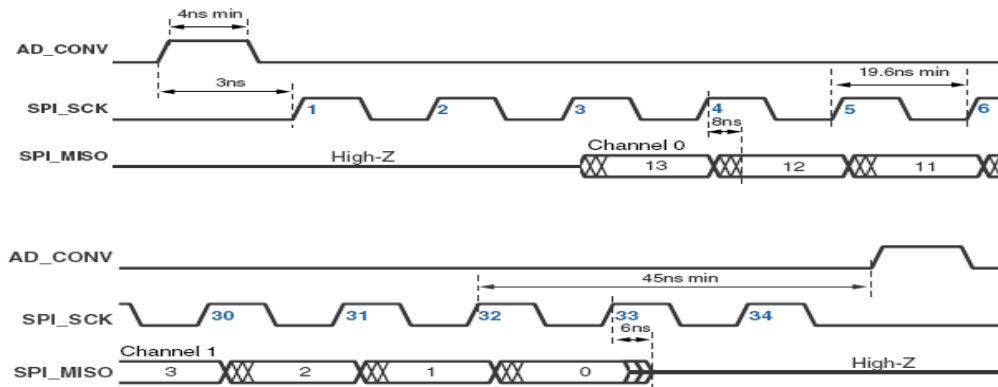


Figure 4.14 Timing diagram of ADC SPI signal [13]

4.5.4 FSM State diagram to interface ADC with FPGA

Moore FSM is designed to meet the timing diagram of the SPI signal of ADC. The ACONV signal is active for minimum of 4 ns to sample the input signal at that particular instant.

and the data starts send to SPI_MISO after two SPI_SCK. And at the end for two clock period MISO is at high impedance state.

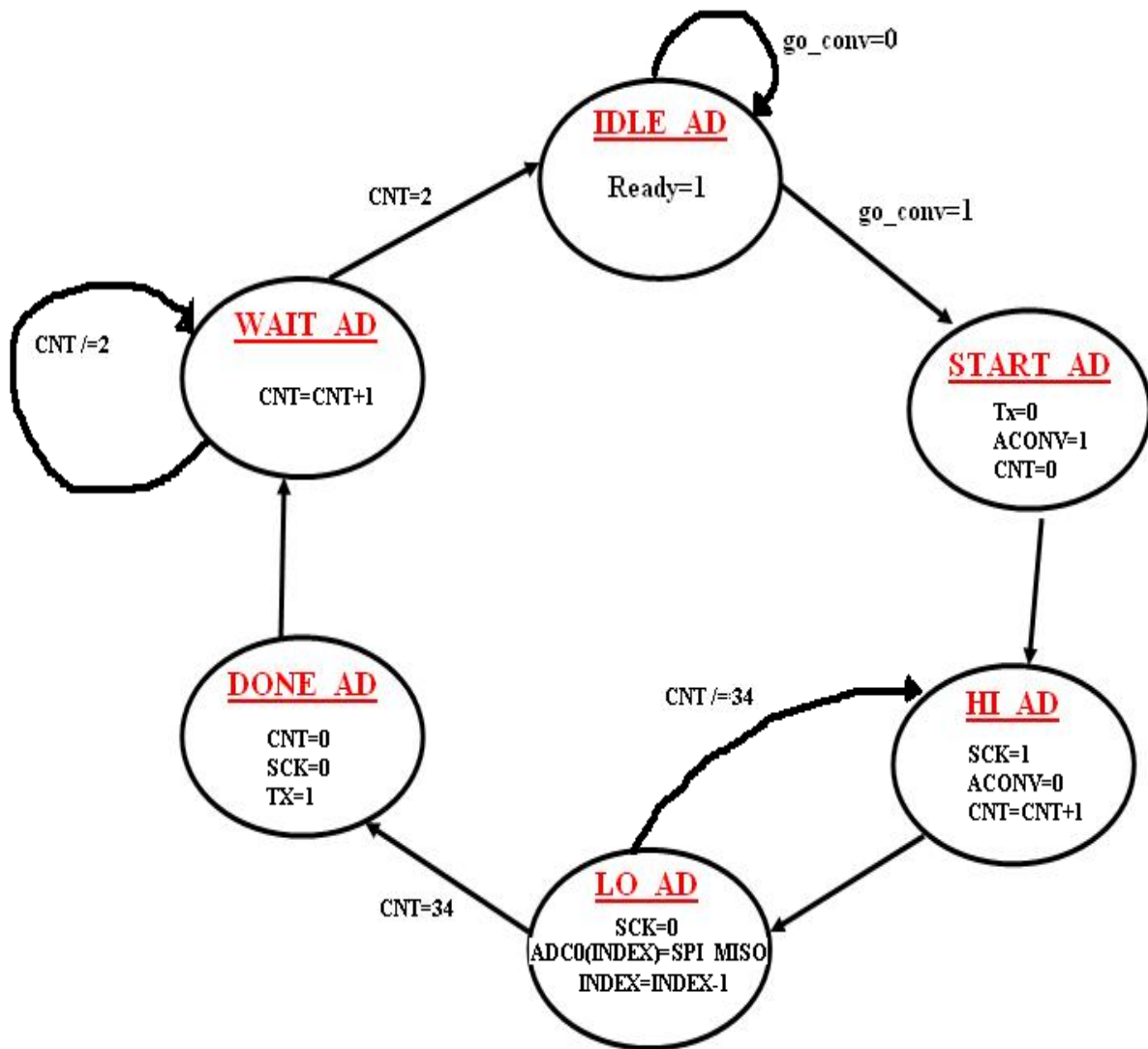


Figure 4.15 FSM for getting data from ADC

4.5.5 RTL schematic of ADC Module

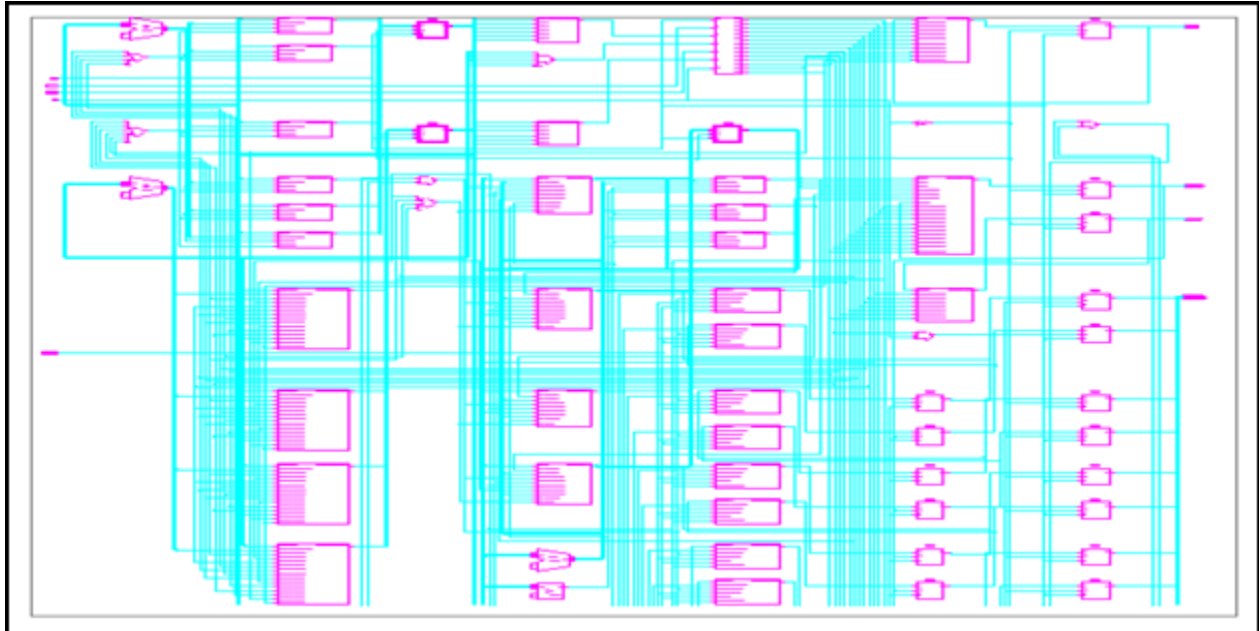


Figure 4.16 RTL schematic of ADC (part 1)

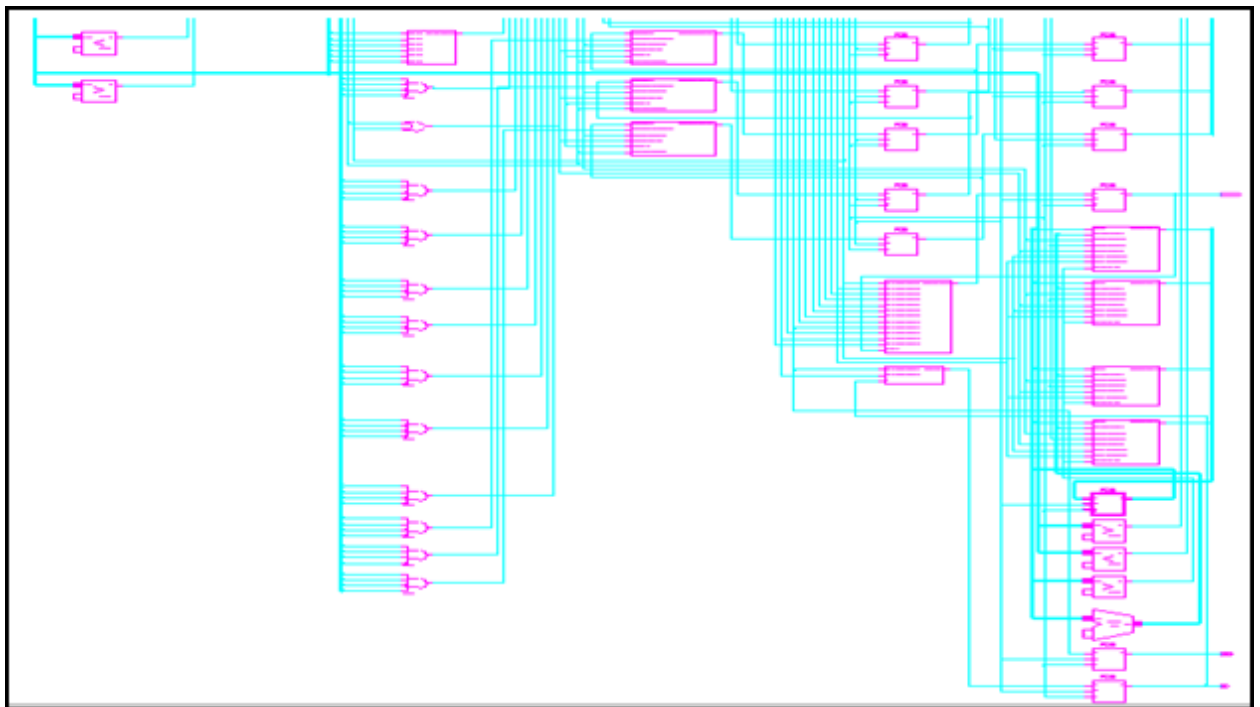


Figure 4.17 RTL schematic of ADC (part 2)

4.5.6 Verification of signal using Chipscope pro

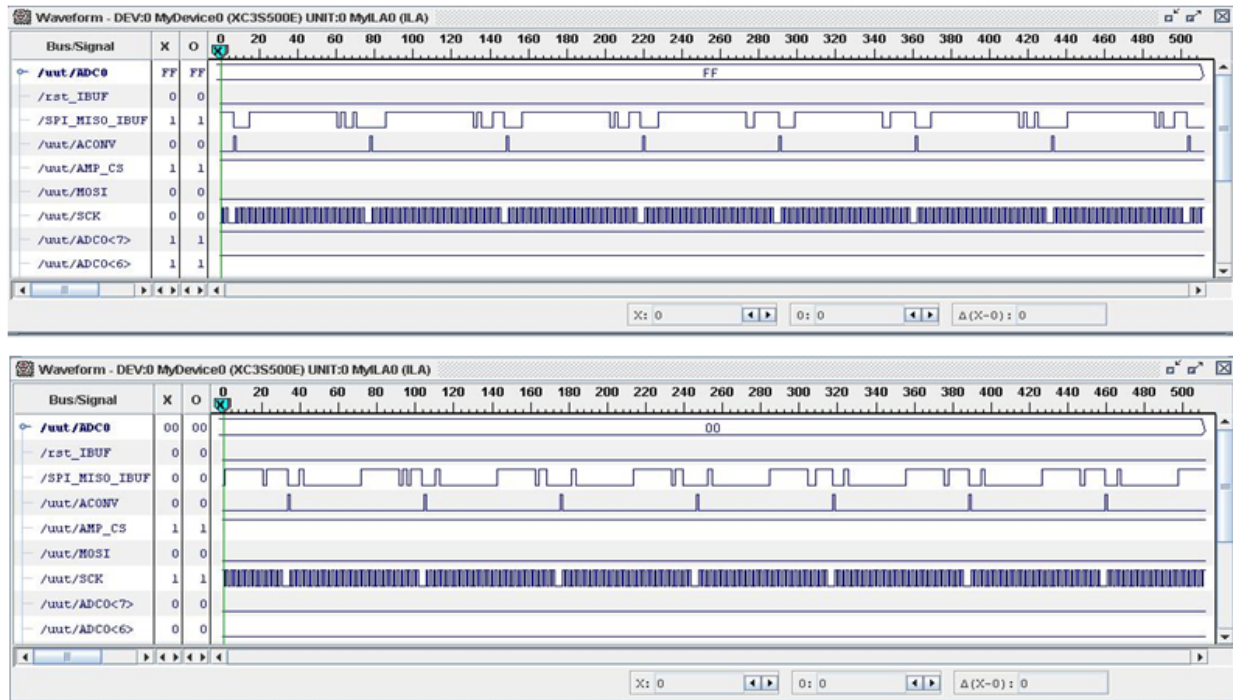


Figure 4.18 Chipscope pro analysis of internal signal of ADC

4.6 ADC-DAC Module

ADC and DAC of the Spartan 3E board are used to test the functionality of ADC. The 14 bit data received from ADC is again converted to 12 bit because DAC take only 12 bit unsigned number. So a top_level module is designed where the ADC and DAC are interfaced together. There is main_control block which control the flow of signal and assign the SPI_SCK and SPI_MISO and SPI_MOSI to one which is active at any time. At a time either ADC or only DAC can work so main_module play a very important role.

4.6.1 RTL schematic of ADC-DAC module

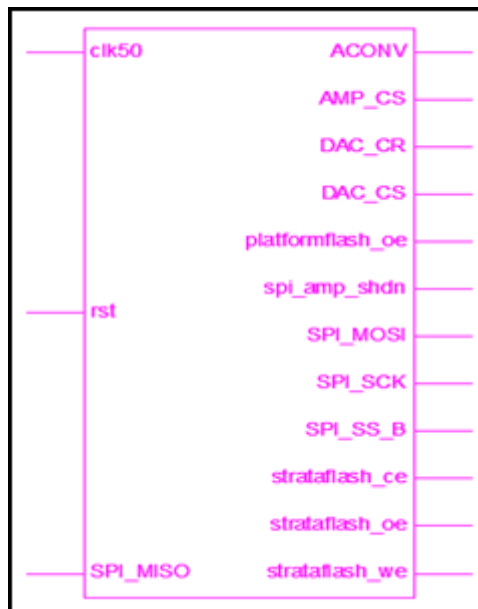


Figure 4.19 Entity of top level module

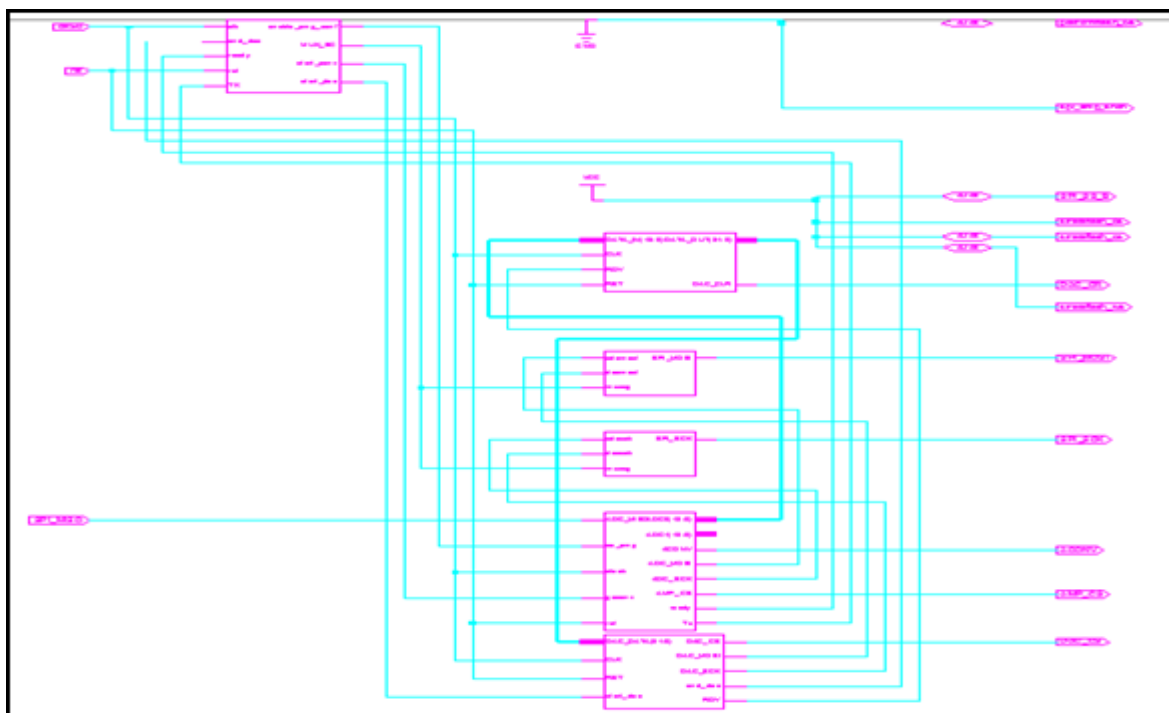


Figure 4.20 RTL schematic of TOP_level module

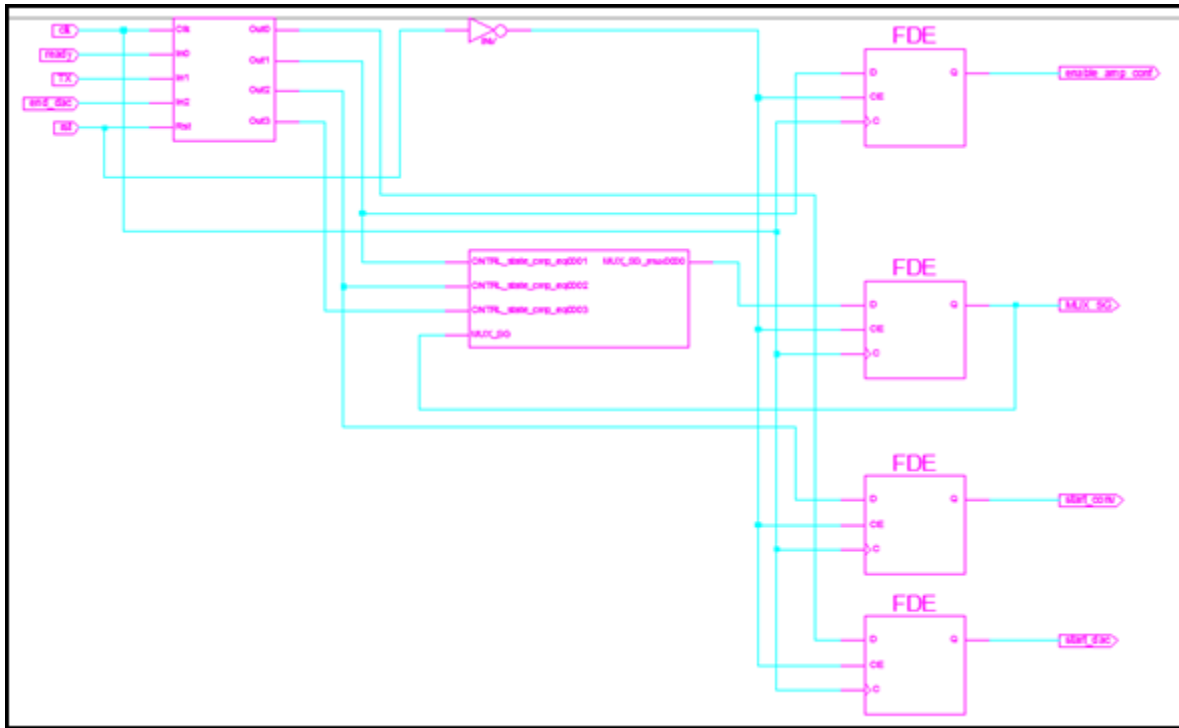


Figure 4.21 RTL schematic of Main_ctrl

4.6.2 Experimental set-up of ADC-DAC

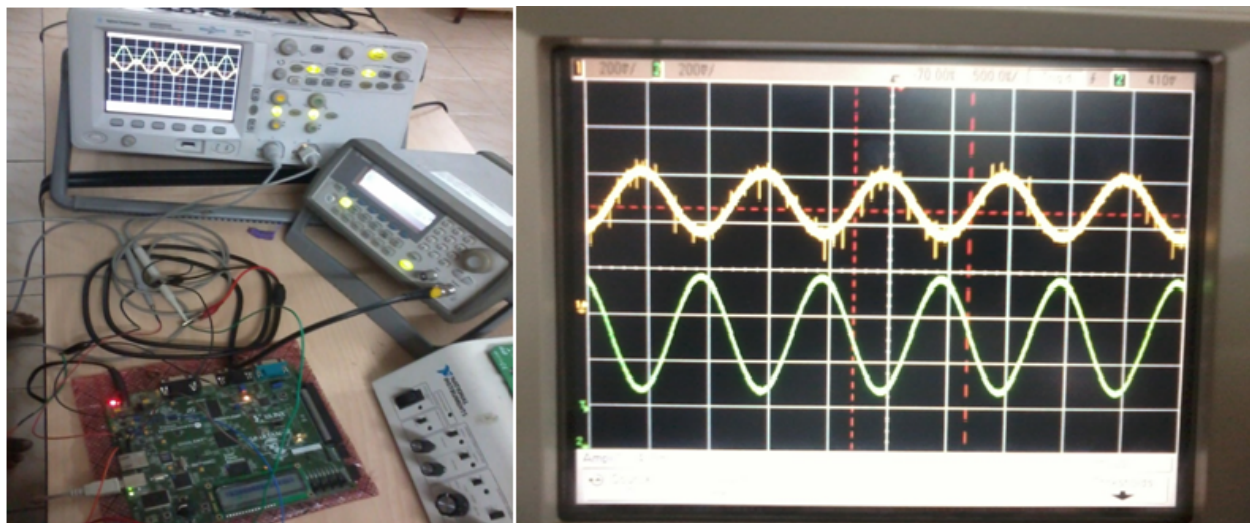


Figure 4.22 Experimental set-up for ADC-DAC

4.7 Controller for Fuel cell power system

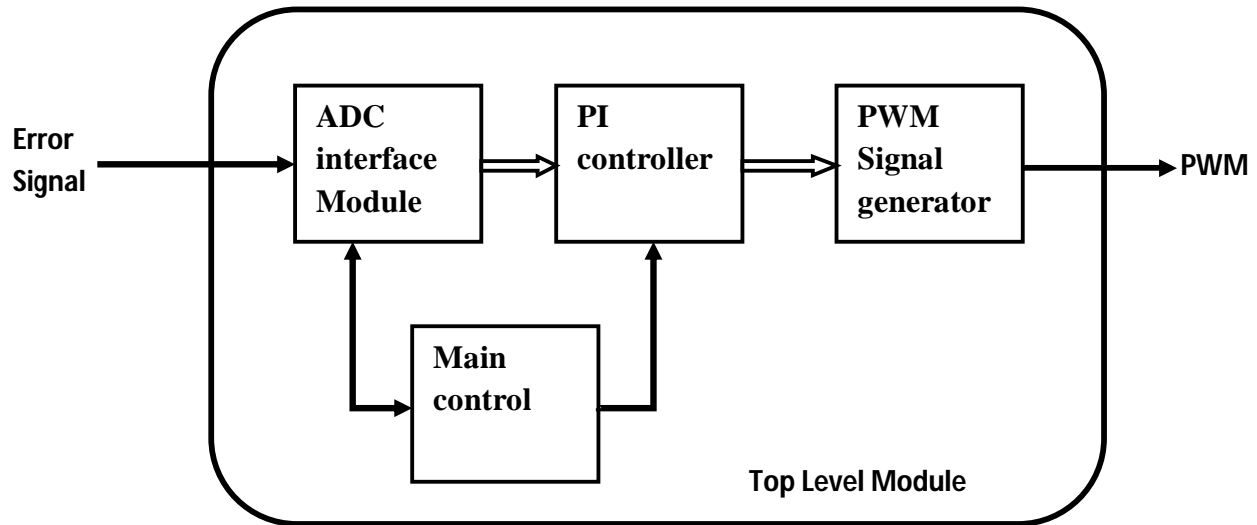


Figure 4.23 Block diagram of controller for Fuel cell

4.7.1 Analysis of PI and PWM with ADC using Chipscope Pro

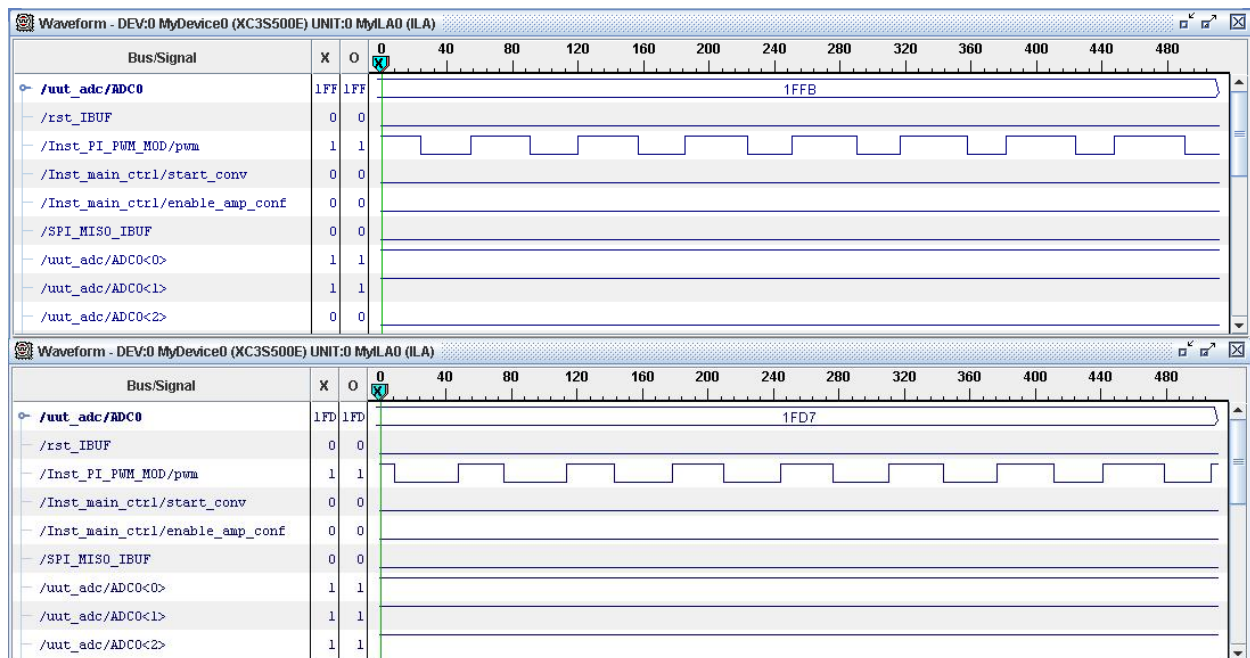


Figure 4.24 PWM out signal analysis using chipscope pro

4.7.2 Design summary of PI and PWM using ADC

Table 4.5 Design Summary of PI and PWM using ADC

Logic Utilization	Used	Available	Utilization
Total no. of slice Register	388	9312	4%
No. of flip flop	382	9312	4%
No. of latches	6		
No. of 4 input LUTs	707	9312	7%
No. of Occupied slices	536	4656	11%

4.7.3 Experimental set-up



Figure 4.25 Experimental set-up for PI and PWM using ADC

4.8 Summary

Control strategy for a fuel cell system using PI controller and PWM signal generator has been implemented. Error signal generated which is analog is to interface with a digital controller synthesized in FPGA is done by an ADC module available in Spartan 3E board. Maximum sampling rate that can be achieved is 1.5 MHz which is sufficient for this type of application.

Chapter 5

Hardware

Implementation of

Fuel cell controller

Chapter 5 : HARDWARE IMPLEMENTATION OF FUEL CELL CONTROLLER

The power conditioning unit which contains a DC converter stage, and control switching which is a feedback path making it a close loop system. A buck-boost converter is designed with L value 8 mH; C is 100 uF; load of 20 ohm. It works well in an open loop till the load and power supply is constant. We desire for a constant power supply which need a close loop system. The voltage is sampled using a voltage divider circuit and it becomes input to the feedback path which is then subtracted from a desired value and signal generated is error signal. Now we optimize the error by a PI controller which is designed in the FPGA using VHDL. The PI output will be the reference to the PWM which decide the duty cycle of the switching pulse.

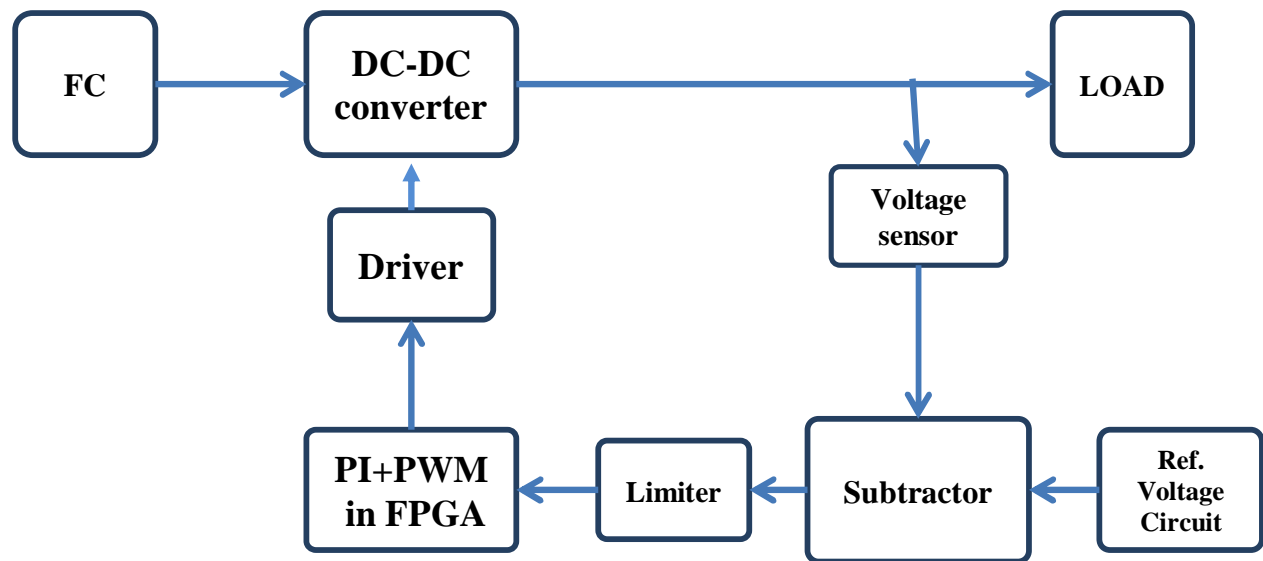


Figure 5.1. Power conditioning unit for Fuel Cell

5.1 Sub block of PCU (Power Conditioning Unit)

Different sub blocks of the power conditioning unit are:

- Buck-Boost circuit.
- Voltage sensor circuit.
- Subtractor circuit.
- Limiter (or clipper) circuit.
- Controller (PI and PWM signal generator) implemented in FPGA.
- Driver circuit.

Buck boost circuit is designed and simulated in MATLAB/SIMULINK and then was realized in hardware. Voltage sensor is a simple voltage divider circuit using two resistor. Subtractor circuit is designed using an Op-amp which gives the difference between the two inputs.

5.1.1 Subtractor circuit:

A Subtractor is an electronic circuit which gives a difference of the input voltage. Subtractor is been designed using a Op-amp (UA741). Output Voltage equation

$$V_{out} = V_2 - V_1 \quad (1)$$

Where $R_1 = R_2 = R_3 = R_4$

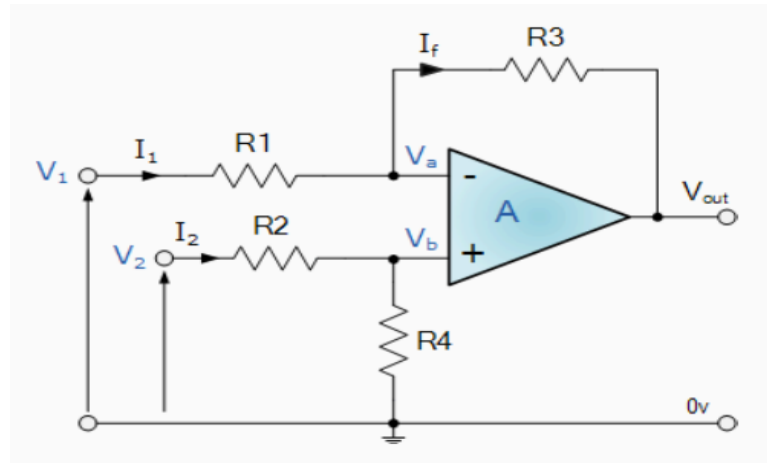


Figure 5.2 Op-amp based subtractor circuit

5.1.2 Limiter (or Clipper) circuit

It is a clipper circuit implemented using two diode and voltage source. The upper and lower limit outputs of the circuit or the clipping point are decided by the voltage source connected with diodes.

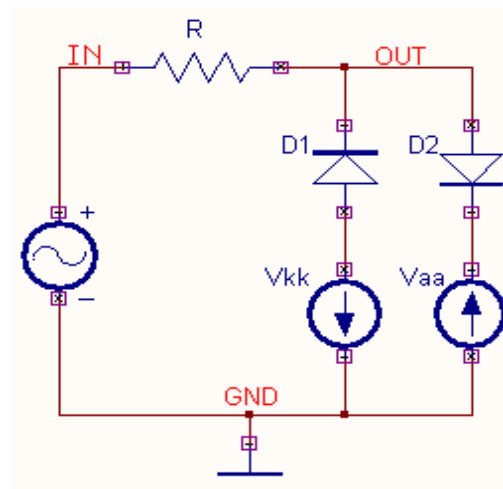


Figure 5.3 Schematic diagram of Limiter circuit

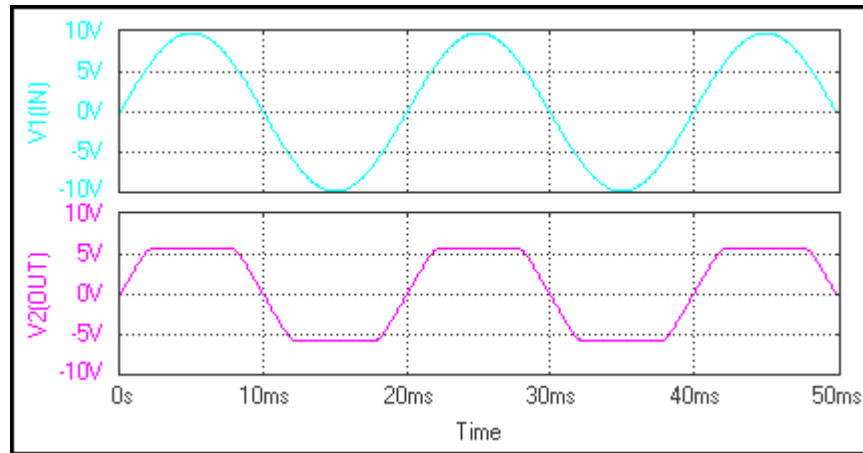


Figure 5.4 Waveform output of Limiter circuit

5.1.3 Driver circuit

Driver circuit provides the isolation of the PWM signal generated from the FPGA to the power MOSFET switch. It also satisfies the current need of the demand by the MOSFET switch for switching in between saturation and cut-off region. A Gate driver circuit which has to provides the desired voltage and current to gate for the switching, and also provide isolation. Using an Opto-Coupler (HCPL817) it has been done which suitable to our need with less need of component and low power consumption.

Specification of HCPL817

- High input-output isolation voltage
- Response time(4 μ s)
- Compact dual-in-line package

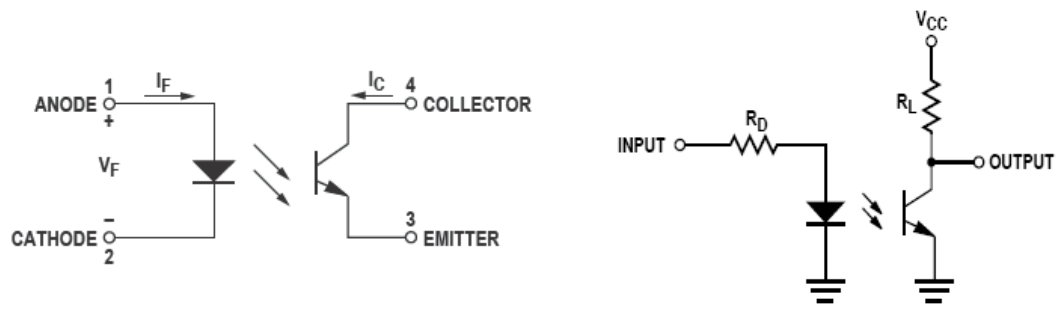


Figure 5.5 Opto Coupler internal schematic of (HCPL817)

5.3 Experimental Set-up

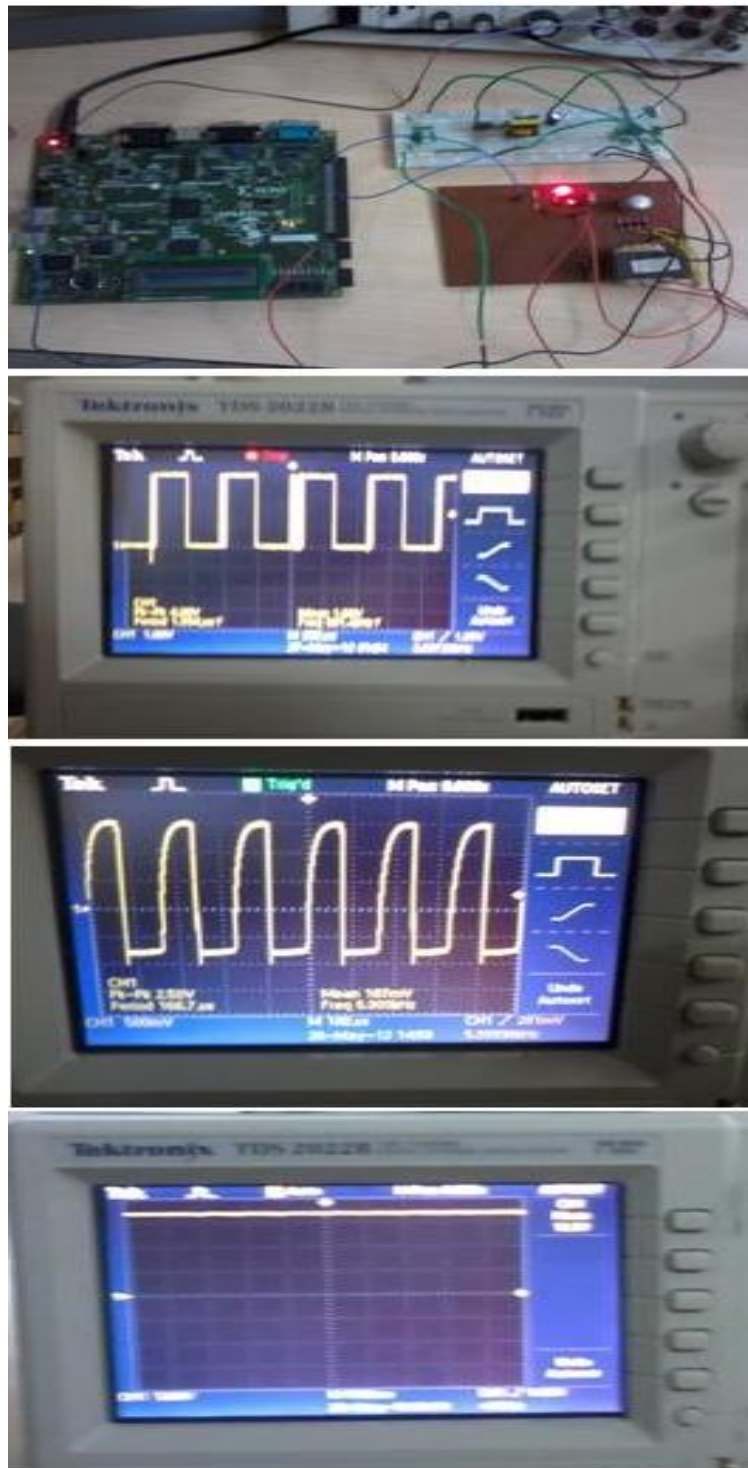


Figure 5.6 Complete Circuit for Fuel Cell

5.4 Summary

The hardware set-up made for the fuel cell controller where a dc voltage source was taken in place of fuel cell. And a 16 V unstable source was made using a rectifier and simple capacitor filter and a desired 12 V constant was generated. We need a small resistance in series with the inductor so it generate voltage drop across it.

Chapter 6 CONCLUSION

The proposed digital controller is able to control the output of any renewable energy sources. A method to synthesized controller for fuel cell power system is developed using VHDL. The proposed method is simulated, and the results demonstrate appropriate performance of the system and controllers. Initially the system were simulated in MATLAB/SIMULINK, to make a reference for VHDL implementation, after the MATLAB/SIMULINK modeling, controller for fuel cell system model has developed in VHDL by using some approximation and assumption. A working hardware has allowed to prototype hardware for fuel cell controller.

Chapter 7 FUTURE WORK

In this dissertation, I have implemented a FPGA based PI controller and a PWM signal generator to control switch the dc-dc converter for a stable power supply from fuel cell to any dc application. We can use a fuzzy controller which takes into account both error and rate of change of error; which can may the system more stable and quicker. For the AC application or to have grid connection we need to implement a DC-AC inverter and a sinusoidal PWM generator as the controller strategy. HCC controller which has much more benefits can also be implemented in inverter control strategy.

Chapter 8 REFERENCES

- [1] A. Kirubakaran , Shailendra Jain, R.K. Nema, “A review on fuel cell technologies and power electronic interface,” *Renewable and Sustainable Energy Reviews 13 (2009) 2430–2440*.
- [2] Boudghene SA, Traversa E. “Fuel cells, an alternative to standard sources of energy”. *Renew Sustain Energy Rev* 2002;6:297–306.
- [3] Huang X, Zhang Z, Jiang J. Fuel cell technology for distributed generation: an overview. In: *IEEE Symposium on Industrial Electron*. 2006. p. 1613–8.
- [4] Ellis MW, Von Spakovsky MR, Nelson DJ. Fuel cell systems: efficient flexible energy conversion for the 21st century. *IEEE Proc* 2001;89:1808–18.
- [5] Farooque M, Maru HC. Fuel cells—the clean and efficient power generators. *IEEE Proc* 2001;89:1819–29.
- [6] Blaabjerg F, Chen Z, Kjaer SB. Power electronics as efficient interface in dispersed power generation systems. *IEEE Trans Power Electron* 2004;19:1184-94.
- [7] http://en.wikipedia.org/wiki/DC-to-DC_converter.
- [8] Muhammad H. Rashid, *Power Electronics Handbook, Academic Press, US*.
- [9] Zhenhua Jiang and Roger A. Dougal, “A Compact Digitally Controlled Fuel Cell/Battery Hybrid Power Source”, *Ieee transactions on industrial electronics, vol. 53, no. 4, august 2010*
- [10] Siriroj Sirisukprasert and Trin Saengsuwan, "The Modeling and Control of Fuel Cell Emulators", *Proceedings of ECTI-CON 2010*.

- [11] K. Petrinec, M. Cirstea, , K. Seare, C. Marinescu “A Novel FPGA Fuel Cell System Controller Design”.11th International conference on Optimization of Electrical and Electronic Equipmen,2008, pp. 401-406.
- [12] C. Boccaletti, G. Fabbri, O. Riot, E. Santini,"Modeling and simulation of hybrid SOFC-GT systems for Distributed Generation“, "La Sapienza"Via Eudossiana 18, 00184 Rome, Italy.
- [13] WWW.xilinx.com,"Spartan-3E Starter Kit Board User Guide",UG230 (v1.0) March 9, 2006.
- [14] Abhishek Sakhare , Asad Davari , *Ali Feliachi* , “Fuel cell for stand-alone and grid connection”, Journal of Power Sources 135 (2009) 165–176.